

Targeted Therapies for Diabetes: DNA Damage, Epigenetic Modifications, and Oxidative Stress

Lead Guest Editor: Shikha Tewari

Guest Editors: Julia Dos Santos and Thiago Gomes Heck





Targeted Therapies for Diabetes: DNA Damage, Epigenetic Modifications, and Oxidative Stress

**Targeted Therapies for Diabetes: DNA
Damage, Epigenetic Modifications, and
Oxidative Stress**

Lead Guest Editor: Shikha Tewari


Guest Editors: Julia Dos Santos and Thiago Gomes
Heck




Copyright © 2023 Hindawi Limited. All rights reserved.

This is a special issue published in "Journal of Diabetes Research." All articles are open access articles distributed under the Creative Commons Attribution License, which permits unrestricted use, distribution, and reproduction in any medium, provided the original work is properly cited.

Chief Editor

Mark Yorek , USA

Associate Editors


Bright Starling Emerald , United Arab Emirates

Christian S. Goebel , Austria

Andrea Scaramuzza , Italy

Akira Sugawara , Japan


Academic Editors

E. Adeghate , United Arab Emirates

Abdelaziz Amrani , Canada


Michaela Angela Barbieri , Italy

Virginia Boccardi, Italy


Antonio Brunetti , Italy


Riccardo Calafiore , Italy

Stefania Camastra, Italy

Ilaria Campesi , Italy


Claudia Cardoso , Brazil


Sergiu Catrina , Sweden

Subrata Chakrabarti , Canada


Munmun Chattopadhyay , USA

Eusebio Chiefari, Italy

Mayank Choubey , USA

Secundino Cigarran , Spain


Huantian Cui, China

Rosa Fernandes , Portugal


Andrea Flex, Italy


Daniela Foti , Italy

Georgia Fousteri , Italy


Maria Pia Francescato , Italy

Pedro M. Geraldes, Canada

Almudena Gómez-Hernández , Spain


Eric Hajduch , France

Gianluca Iacobellis , USA

Carla Iacobini , Italy

Marco Infante , USA

Sundararajan Jayaraman, USA

Guanghong Jia , USA

Niki Katsiki , United Kingdom


Daisuke Koya, Japan

Olga Kozłowska, United Kingdom

Manishekhar Kumar, USA

Lucy Marzban, Canada

Takayuki Masaki , Japan

Raffaella Mastrocola , Italy

Maria Mirabelli , Italy


Ramkumar Mohan, USA

Pasquale Mone , USA

Craig S. Nunemaker , USA

Emmanuel K Ofori, Ghana

Hiroshi Okamoto, Japan

Ike S. Okosun , USA

Driss Ousaaid , Morocco

Dario Pitocco, Italy

Balamurugan Ramatchandirin, USA

Asirvatham Alwin Robert, Saudi Arabia

Saheed Sabiu , South Africa

Toshiyasu Sasaoka, Japan

Adérito Seixas , Portugal

Viral Shah , India

Ali Sharif , Pakistan

Ali Sheikhy, Iran

Md. Hasanuzzaman Shohag, Bangladesh

Daniele Sola , Italy

Marco Songini, Italy

Janet H. Southerland, USA

Vincenza Spallone , Italy

David Strain, United Kingdom

Bernd Stratmann , Germany

Farook Thameem, USA






Kazuya Yamagata, Japan

Liping Yu , USA

Burak Yulug, Turkey

Contents

Epigenetic Changes Induced by High Glucose in Human Pancreatic Beta Cells

Rasha A. Alhazzaa , Raechel E. McKinley, Bruk Getachew , Yousef Tizabi , Thomas Heinbockel , and Antonei B. Csoka 




Research Article (15 pages), Article ID 9947294, Volume 2023 (2023)

Oxidative and Cellular Stress Markers in Postmenopause Women with Diabetes: The Impact of Years of Menopause

Carolain Felipin Vincensi Anklam, Yana Picinin Sandri Lissarassa, Analú Bender dos Santos, Lílian Corrêa Costa-Beber, Lucas Machado Sulzbacher, Pauline Brendler Goettens-Fiorin, Thiago Gomes Heck , Matias Nunes Frizzo, and Mirna Stela Ludwig 

Research Article (9 pages), Article ID 3314871, Volume 2021 (2021)

ROS-ERK Pathway as Dual Mediators of Cellular Injury and Autophagy-Associated Adaptive Response in Urinary Protein-Irritated Renal Tubular Epithelial Cells

Jian-kun Deng, Xueqin Zhang , Hong-luan Wu, Yu Gan, Ling Ye, Huijuan Zheng, Zebing Zhu, Wei Jing Liu , and Hua-feng Liu 

Research Article (8 pages), Article ID 6614848, Volume 2021 (2021)

Research Article

Epigenetic Changes Induced by High Glucose in Human Pancreatic Beta Cells

Rasha A. Alhazzaa ^{1,2}, Raechel E. McKinley,¹ Bruk Getachew ³, Yousef Tizabi ³,
Thomas Heinbockel ¹ and Antonei B. Csoka ¹

¹Department of Anatomy, Howard University, 520 W St. NW, Washington DC 20059, USA

²King Saud bin Abdulaziz University for Health Sciences, Riyadh 14611, Saudi Arabia

³Department of Pharmacology, Howard University, 520 W St. NW, Washington DC 20059, USA

Correspondence should be addressed to Antonei B. Csoka; antonei.csoka@howard.edu

Received 5 April 2021; Revised 4 December 2021; Accepted 7 July 2022; Published 13 February 2023

Academic Editor: Thiago Heck

Copyright © 2023 Rasha A. Alhazzaa et al. This is an open access article distributed under the Creative Commons Attribution License, which permits unrestricted use, distribution, and reproduction in any medium, provided the original work is properly cited.

Epigenetic changes in pancreatic beta cells caused by sustained high blood glucose levels, as seen in prediabetic conditions, may contribute to the etiology of diabetes. To delineate a direct cause and effect relationship between high glucose and epigenetic changes, we cultured human pancreatic beta cells derived from induced pluripotent stem cells and treated them with either high or low glucose, for 14 days. We then used the Arraystar 4x180K HG19 RefSeq Promoter Array to perform whole-genome DNA methylation analysis. A total of 478 gene promoters, out of a total of 23,148 present on the array (2.06%), showed substantial differences in methylation ($p < 0.01$). Out of these, 285 were hypomethylated, and 193 were hypermethylated in experimental vs. control. Ingenuity Pathway Analysis revealed that the main pathways and networks that were differentially methylated include those involved in many systems, including those related to development, cellular growth, and proliferation. Genes implicated in the etiology of diabetes, including networks involving glucose metabolism, insulin secretion and regulation, and cell cycle regulation, were notably altered. Influence of upstream regulators such as MRTFA, AREG, and NOTCH3 was predicted based on the altered methylation of their downstream targets. The study validated that high glucose levels can directly cause many epigenetic changes in pancreatic beta cells, suggesting that this indeed may be a mechanism involved in the etiology of diabetes.

1. Introduction

Diabetes mellitus (DM) is a chronic metabolic disease in which either the pancreas produces very little or no insulin, or the target cells of the body do not respond correctly to the insulin produced, resulting in high levels of glucose in the blood and urine. DM is associated with both genetic and environmental factors. The cost of treating it and its complications has considerably increased because of an epidemic of DM worldwide [1].

Epigenetics is a term used to describe heritable (somatic or meiotic) changes in gene expression not caused by changes in the DNA sequence, resulting in alterations in

the way cells “read” or express genes. Additionally, epigenetics relates to a causal chain linking genetics, environmental exposure, and disease development. Epigenetic changes occur often during an organism’s lifetime and may be transmitted to the next generation [2]. Also, numerous factors may cause epigenetic changes, such as breastfeeding and maternal care, physical activity or inactivity, hyperglycemia, mitochondrial dysfunction, aging, and menopause [2]. Epigenetic state may even be influenced by pharmaceutical drugs [3] and integrative medicine [4].

Three major epigenetic systems are the focus of current research: DNA methylation, covalent posttranslational modification to histones (i.e., methylation, phosphorylation,

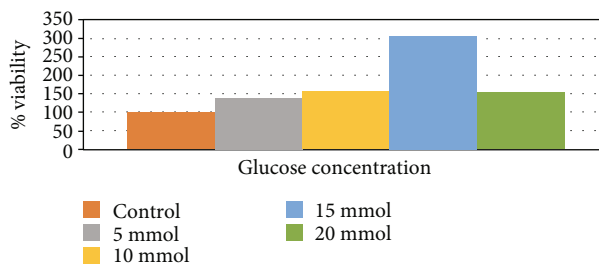


FIGURE 1: % Cell viability using MTT assay. No negative effect was observed on cell morphology or growth kinetics at or below 15 mM, but at a concentration of 20 mM, a cytotoxic effect was noted. A 15 mM solution of glucose was determined to be the maximum concentration that could be used without inducing cell death.

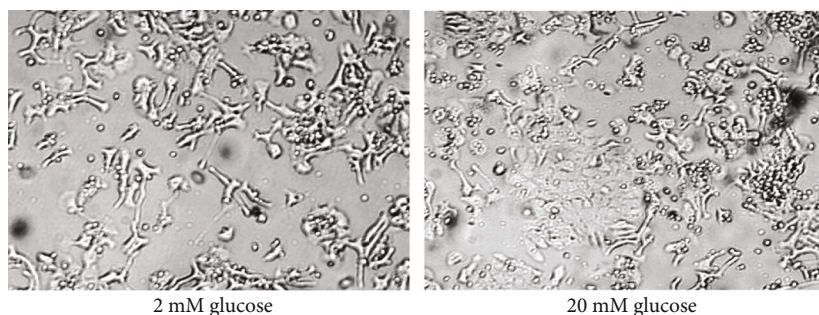


FIGURE 2: Cell morphology and cell death. Images of hiPS beta cells in concentrations of glucose of 2 mM and 20 mM. It was noticed that there was a difference in cellular morphology between the high- and low-glucose groups, indicative of increased cell death at the higher concentration.

acetylation, and ubiquitylation), and noncoding RNAs (ncRNAs) that modify gene expression at the transcriptional and posttranscriptional stages.

Several studies have already suggested that epigenetics plays a significant role in the etiology of DM, in particular T2D [5–8]. Also, the changes in T2D, such as chronic hyperglycemia, hypoxia, increased oxidative stress, and dyslipidemia, could both result from, and cause, epigenetic alterations associated with the disease [8–10]. Furthermore, it is known that hypoxia influences several precursor cell types' stemness and lineage commitment during development, including pancreatic beta cells [11]. *In vivo*, beta cell neogenesis is negatively regulated by hypoxia-inducible factor 1 alpha (HIF-1 α) caused by low oxygen tension [12]. It has also been found that repression of HIF-1 α causes increased development of Ngn3-positive endocrine progenitors, resulting in higher levels of beta cell neogenesis and growth [12]. Furthermore, the deletion of the von Hippel-Lindau (VHL) gene, which encodes a protein involved in the degradation of HIF-1 α , leads to compromised beta cell development. This will have a further negative impact on beta cell neogenesis [13]. Furthermore, Sun et al. found that hypoxia (2% pO₂) directly affects the differentiation of mesenchymal stem cells into early beta cell progenitors [14].

The principal insulin-producing cells in the pancreas are the beta cells, and epigenetic tags play a crucial role in establishing and sustaining their functional identity [9]. Stable beta cell function is critical for the regulation of glucose levels in the blood. In contrast, epigenetic dysregulation results in decreased expression of genes essential for beta cell

function, the inappropriate activation and expression of genes that should normally remain repressed, and compromised genetic imprinting, resulting in loss of beta cell identity [9] and reduced insulin secretion [6].

The origin of an altered epigenetic state in beta cells in DM has not been fully elucidated. Beta cells could be an especially sensitive target in prediabetes and related conditions, because not only do they produce insulin, but also respond to insulin and glucose levels themselves. To directly test the hypothesis that a high glucose environment, characteristic of prediabetes, can cause epigenetic changes, we wanted to establish a direct cause and effect link between high glucose levels and an altered epigenetic state in the cells. Therefore, we treated beta cells differentiated from induced pluripotent stem cells (iPSCs) with high (15 mM) vs. low (2 mM) glucose and looked for epigenetic changes by performing genome-wide DNA methylation analysis. We also investigated affected signaling pathways and gene networks, including those thought to be involved in the etiology of DM. Our hypothesis was that a high glucose concentration would cause significant genome-wide epigenetic changes in pancreatic beta cells and that this dynamic could promote the development of DM.

2. Materials and Methods

2.1. Cell Culture. For this study, Cellartis hiPS Beta Cells (Takara Bio, CA, USA) were used to investigate beta cell activity. The benefits of using these cells are that they can be conveniently used instead of pancreatic islets. In some

ways, they are superior to islets because they are pure beta cells and can be used as a physiologically important model for insulin development and release. These cells secrete high amounts of insulin and C-peptide and exhibit significant protein expression of MAFA, NKX6-1, PDX1, and UCN3. Also, they are differentiated from an iPSC cell line, ChiPSC22 (Takara Bio, CA, USA), derived from a single donor.

To grow the cells, 6-well plates (Corning, USA) were coated with Cellartis Beta Cell Coating and cultured in growth medium containing Cellartis Beta Cell Basal Medium and supplemented with Cellartis Beta Cell Supplement (Takara Bio, CA, USA). Cells were incubated and maintained in 5% CO₂ at 37°C.

2.2. MTT Assay. A cell viability and toxicity curve was initially performed on the cells using an MTT assay to determine the optimum glucose concentration that can be tolerated without causing cell death. Cells were grown in growth media containing various amounts of glucose (5 mM, 10 mM, 15 mM, and 20 mM) for 48 hours. From 5 mM to 15 mM, cell proliferation increased, but at 20 mM, it decreased (Figure 1). This decrease corresponded to a visible increase in cell death (Figure 2). We observed a difference in cellular morphology between high and low glucose concentrations during this time, e.g., cell differentiation, death, and detachment. These changes are recapitulated *in vivo*; for example, after being treated with high glucose, beta cells go into neogenesis rather than proliferation. The underlying mechanism for this is an increase in insulin resistance in the beta cell mass and impaired glucose tolerance. In addition, this beta cell functional plasticity contributes to the compensation for an increased insulin demand caused by insulin resistance. The mechanism for reduced beta cell mass in T2D is likely a dramatically increased rate of apoptosis [15]. Also, short-term exposure of beta cells to increasing glucose instigates proliferation in a concentration-dependent manner. Hyperglycemia also inhibits beta cell secretory function which is evident before the apoptosis leads to the decrease in cell mass [16]. We saw all these changes occurring in parallel *in vitro*, and therefore, a 15 mM solution of glucose was the maximum concentration that could be used without inducing cell death. Notably, within the literature, insulin secretion increased significantly at 16.7 mM glucose [17].

2.3. Cell Treatment. The hiPS Beta Cells were thawed, resuspended in Beta Cell Maintenance medium, and plated in culture vessels coated with Beta Cell Coating. We seeded the cells into six-well plates in two groups of three: low and high glucose. Three wells served as low-glucose controls, and three (experimental) wells received high glucose. The control group was maintained throughout in the minimum glucose concentration required for cellular viability and maintenance of enrichment of beta cells (2 mM at the recommendation of Takara Bio). For the first four days, media was changed every 24 hours and all six wells contained 2 mM glucose. On days five to eight, glucose was increased to 10 mM in the three experimental wells. Then, on days nine to fourteen, we gradually increased the glu-

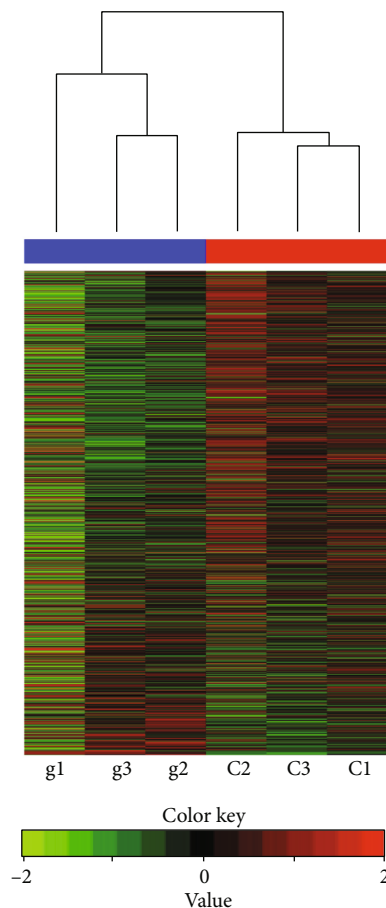


FIGURE 3: Heat map of hypermethylated and hypomethylated gene promoters. MeDIP-Chip analysis grouped into clusters shows the heat map of differentially methylated gene promoters between glucose-treated (g1, g2, and g3) and control-treated (C1, C2, and C3) samples. The scale symbolizes hypomethylated promoters (values 0 to +2) in green and hypermethylated promoters (values 0 to -2) in red. Each tiny row represents a gene on a specified sample signified by columns. There was a clear demarcation between the control samples with most of the genes that are either downregulated (hypermethylated promoters in red) or upregulated (hypomethylated promoters in green) between samples represented in the six rows. The overall methylation clustering between treated and control samples on the top (red and blue) represents quantitative methylation clustering between significant genes.

ose concentration to reach 15 mM in the three experimental wells, to ensure that the cells did not go into shock or glucose toxicity (defined as a temporary physiological condition triggered by frequent or extended exposure to high glucose concentrations) [18].

2.4. DNA Extraction and MeDIP-Chip Analysis. After 14 days, the 2 mM or 15 mM glucose-treated cells were lysed, and genomic DNA (gDNA) was homogenized using Qiasredder (Qiagen, Fremont, CA) and extracted using the DNeasy kit (Qiagen, Fremont, CA). The DNA processing protocol then closely follows our previous paper [19]. The purified gDNA was then quantified, and quality assessed

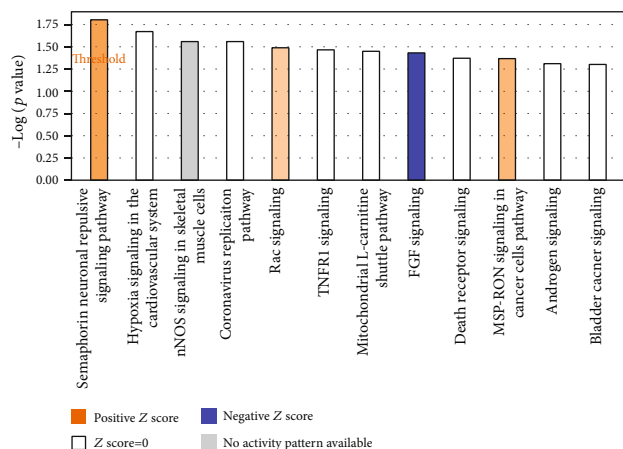


FIGURE 4: Top canonical pathways altered by glucose. The bar graph depicts the main canonical pathways predicted to be altered by high glucose treatment using IPA core analysis. High glucose causes differential methylation of significant genes from our dataset that are enriched in canonical pathways, such as semaphorin neuronal repulsive signaling pathway, hypoxia signaling in the cardiovascular system, nNOS signaling in skeletal muscle cells, coronavirus replication pathway, and Rac signaling based on their z score, ratio, and $-\log(p)$ value. The threshold is set at the lowest level of confidence that is statistically acceptable ($p \leq 0.05$).

by NanoDrop ND-1000. This was followed by sonication to generate fragments of about 200-1000 base pairs. Immunoprecipitation of methylated DNA was performed using BiomagTM magnetic bead-coupled mouse monoclonal antibody against 5-methylcytidine. The immunoprecipitated DNA was eluted and purified by phenol chloroform extraction and ethanol precipitation [19]. The total input and immunoprecipitated DNA were labeled with Cy3- and Cy5-labeled random 9-mers, respectively, and hybridized to the Arraystar 4x180K HG19 RefSeq Promoter Array, which is a multiplex slide with 4 identical arrays per slide, and each array contains 23,148 well-characterized RefSeq promoter regions (from about -1,300 bp to +500 bp of the Transcription Start Sites) totally covered by ~180,000 probes. Scanning was performed by using Agilent Scanner G2505C (Rockville, MD, USA) [19].

2.5. Data Normalization. Again, normalization followed our previous protocol [19]. Raw data was extracted as txt files by Agilent Feature Extraction software. We performed median centering, quantile normalization, and linear smoothing by Bioconductor packages (Ringo, limma, and MEDME) [20]. The enrichment peaks and differentially methylated peaks were analyzed and annotated by NimbleScan software. The user guide and result data formats can be found at http://www.nimblegen.com/downloads/support/NimbleScan_v2p6_UsersGuide.pdf. After normalization, a normalized \log_2 -ratio data (*_ratio.gff file) was created for each sample. From the normalized \log_2 -ratio data, a sliding-window peak-finding algorithm provided by NimbleScan v2.5 (Roche-NimbleGen) was applied to find the enriched peaks with specified parameters (sliding window width: 1,500 bp; mini probes per peak: 2;

Top canonical pathways			
Name	p value	Overlap	
Sulfite oxidation IV	1.88E-02	100.0%	1/1
Mitochondrial L-carnitine shuttle pathway	3.54E-02	12.5%	2/16
nNOS signaling in skeletal muscle cells	3.64E-02	7.7%	3/39
Hypoxia signaling in the cardiovascular system	4.06E-02	5.8%	4/69
Retinoic acid mediated apoptosis signaling	5.50E-02	6.5%	3/46

Top upstream regulators			
Upstream regulators			
Name	p value	Predicted activation	
MRTFA	2.07E-03	+	
AREG	3.24E-03	+	
NOTCH3	3.77E-03	+	
POU5F1	4.06E-03	+	
HNFA1	4.93E-03	+	

Causal network			
Name	p value	Predicted activation	
POU5F1	8.64E-04	+	
MRTFA	2.07E-03	+	
AREG	3.24E-03	+	
NOTCH3	3.77E-03	+	
miR-17-5p (and other miRNAs w/seed AAAGUGC)	7.07E-03	-	

Top diseases and bio functions			
Diseases and disorders			
Name	p value range	# molecules	
Cardiovascular disease	3.40E-02-2.17E-04	24	
Hereditary disorder	2.39E-02-2.17E-04	76	
Organismal injury and abnormalities	3.54E-02-2.17E-04	165	
Connective tissue disorders	3.14E-02-3.51E-04	15	
Developmental disorder	2.39E-02-3.51E-04	56	

Molecular and cellular functions			
Name	p value range	# molecules	
Cellular development	3.32E-02-6.81E-04	28	
Cellular growth and proliferation	3.32E-02-6.81E-04	25	
Cell morphology	3.40E-02-2.04E-03	15	
Cellular assembly and organization	3.11E-02-2.04E-03	13	
Cellular movement	3.20E-02-2.05E-03	28	

Physiological system development and function			
Name	p value range	# molecules	
Reproductive system development and function	2.05E-02-2.04E-03	12	
Cardiovascular system development and function	3.40E-02-4.69E-03	19	
Connective tissue development and function	1.88E-02-5.01E-03	3	
Organ development	3.53E-02-5.01E-03	14	
Tissue development	3.53E-02-5.01E-03	22	

Top toxic functions			
Cardiotoxicity			
Name	p value range	# molecules	
Cardiac arrhythmia	4.65E-01-2.17E-04	6	
Congenital heart anomaly	3.70E-01-7.74E-03	4	
Tachycardia	2.62E-01-8.37E-03	3	
Cardiac disease	4.93E-02-1.88E-02	3	
Cardiac dilation	4.75E-01-3.72E-02	5	

Hepatotoxicity			
Name	p value range	# molecules	
Liver hyperplasia/hyperproliferation	1.80E-00-1.37E-02	50	
Liver steatosis	7.30E-02-7.30E-02	1	
Liver inflammation/hepatitis	3.72E-01-9.48E-02	5	
Hepatocellular carcinoma	5.04E-01-1.92E-01	17	
Liver cholestasis	4.12E-01-4.12E-01	1	

Nephrotoxicity			
Name	p value range	# molecules	
Glomerular injury	1.00E-00-1.88E-02	4	
Renal damage	4.12E-01-4.12E-01	2	
Renal inflammation	1.00E-00-4.23E-01	2	
Renal nephritis	1.00E-00-4.23E-01	2	
Renal hydropnephrosis	4.65E-01-4.65E-01	1	

Top networks			
ID	Associated network functions	Score	
(1)	Cellular development, Cellular growth and proliferation, cancer	39	
(2)	Gastrointestinal disease, inflammatory disease, inflammatory response	19	
(3)	Cell death and survival, embryonic development, organismal injury and abnormalities	17	
(4)	Cell-to-cell signaling and interaction, hematological system development and function, immune cell trafficking	14	
(5)	Cell death and survival, cell cycle, ophthalmic disease	12	

Top analysis-ready molecules			
Expr p value	Molecules	Value	Chart
	ITPKC	8.91E-05	
	ODF3L1	8.91E-05	
	UPK3B	1.58E-04	
	LOC101927100	1.62E-04	
	HCRT	2.04E-04	
	CLDN3	2.45E-04	
	CLAR	2.82E-04	
	CYTH2	3.98E-04	
	WAS	3.98E-04	
	HESS	4.07E-04	

FIGURE 5: IPA analysis. An initial analysis of canonical pathways, upstream regulators, diseases and biological functions, toxicological functions, networks, and analysis-ready molecules using IPA's core analysis function.

p value minimum cutoff: 2; maximum spacing between nearby probes within peak: 500 bp). After getting the *_peaks.gff files, the identified peaks were mapped to genomic feature transcripts [19].

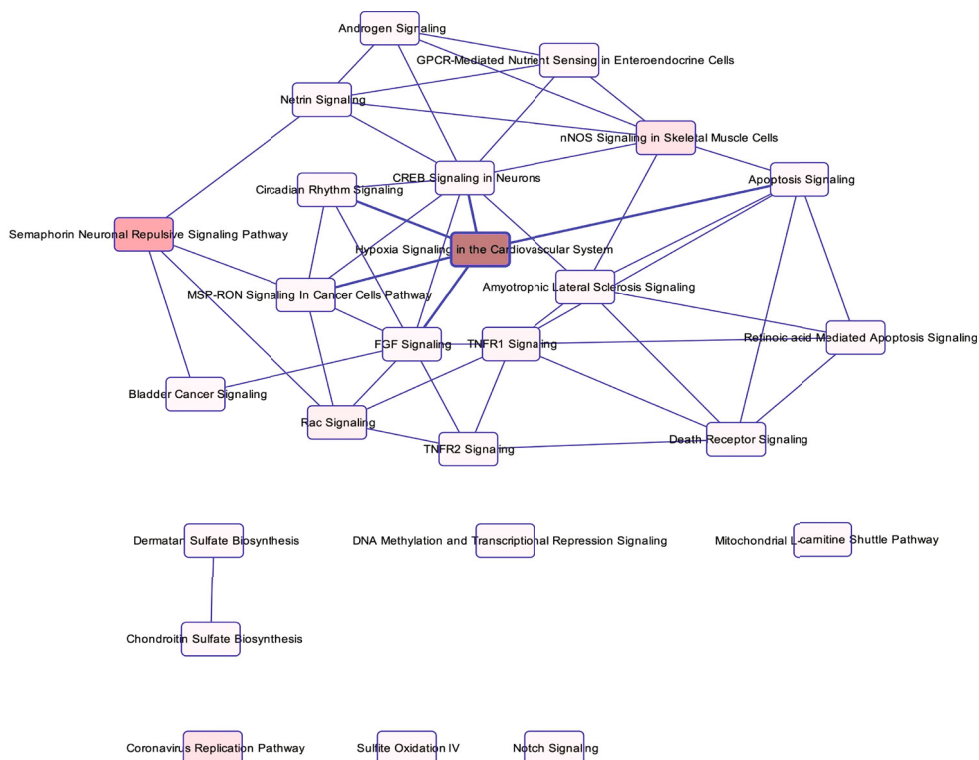


FIGURE 6: Connections between pathways. This figure shows many connected pathways, which means that most of the significantly altered genes are shared between them.

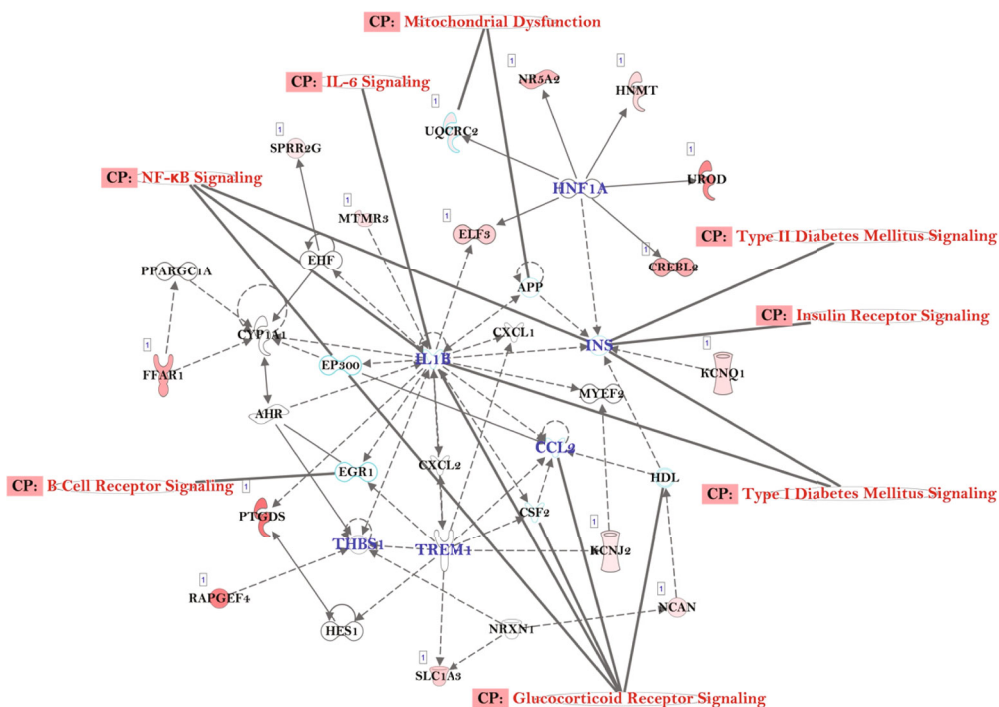


FIGURE 7: IPA analysis identifying the main networks of differentially expressed genes and canonical pathways that contribute to the etiology of DM. Genes are presented with significant effectors on expression pattern with ≥ 2.0 fold change and p value < 0.05 . Dotted lines connecting the genes represent indirect connections, while the straight lines represent directly connecting genes and related pathways.

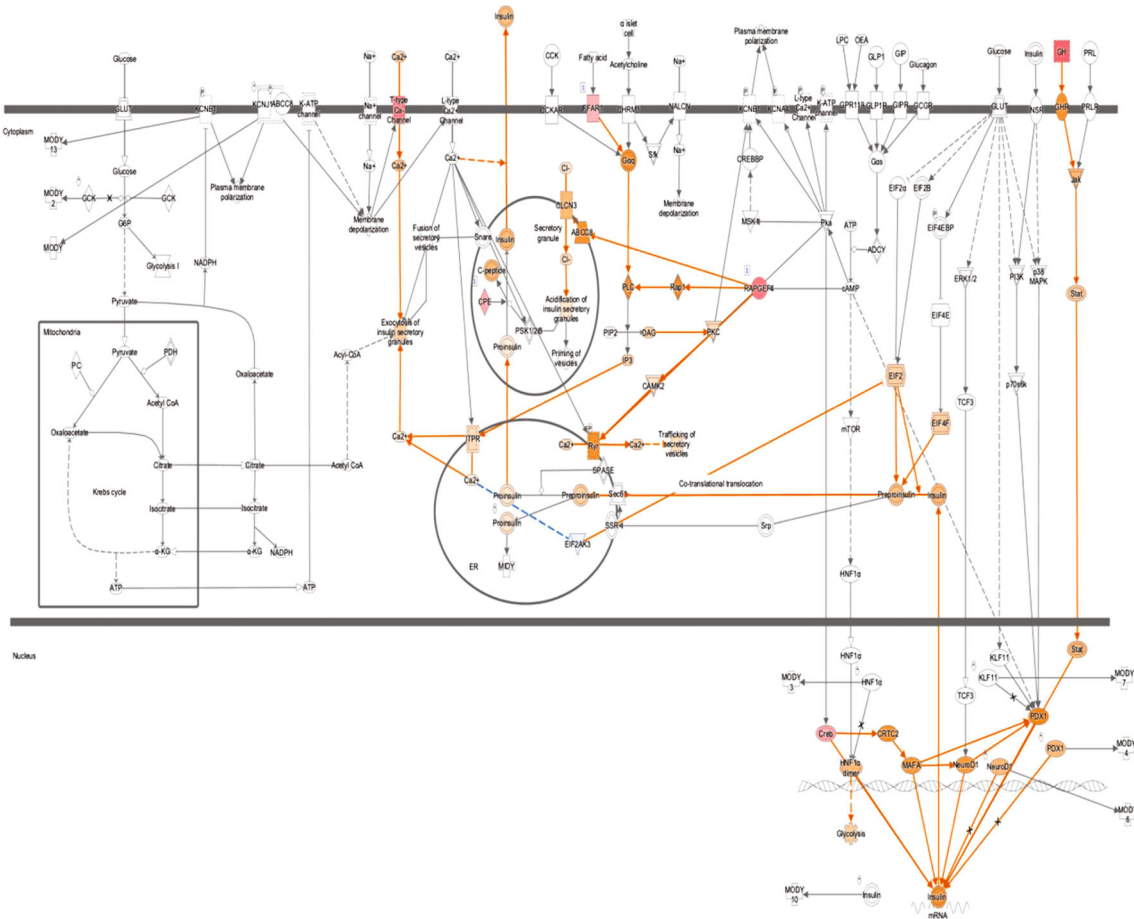


FIGURE 8: Insulin secretion signaling pathway and upregulated molecules. CPE, Creb, FFAR1, RAPGFF4, and T-Type-Ca Channel are upregulators that activate many genes, while ELF2AK3 mostly inhibits.

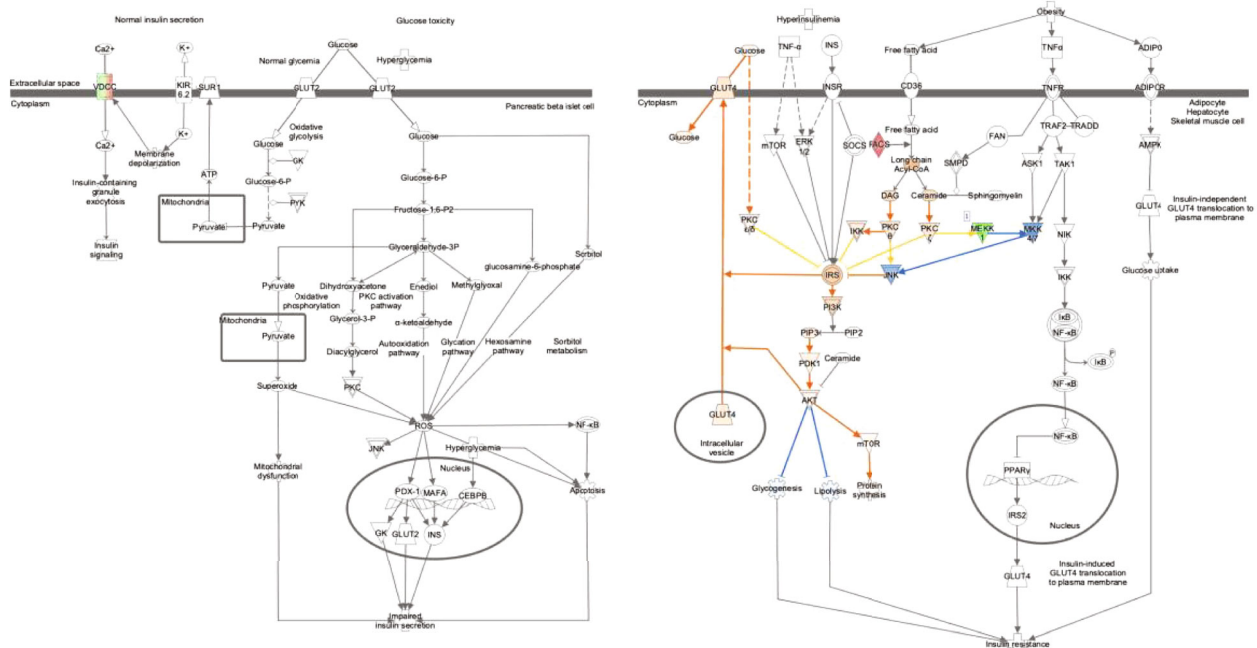


FIGURE 9: T2D signaling and upregulated molecules. GLUT4, IRS, DAG, and AKT are significant metabolic pathways that activate many genes, while MKK 4/7 and JNK play a role in inhibition.

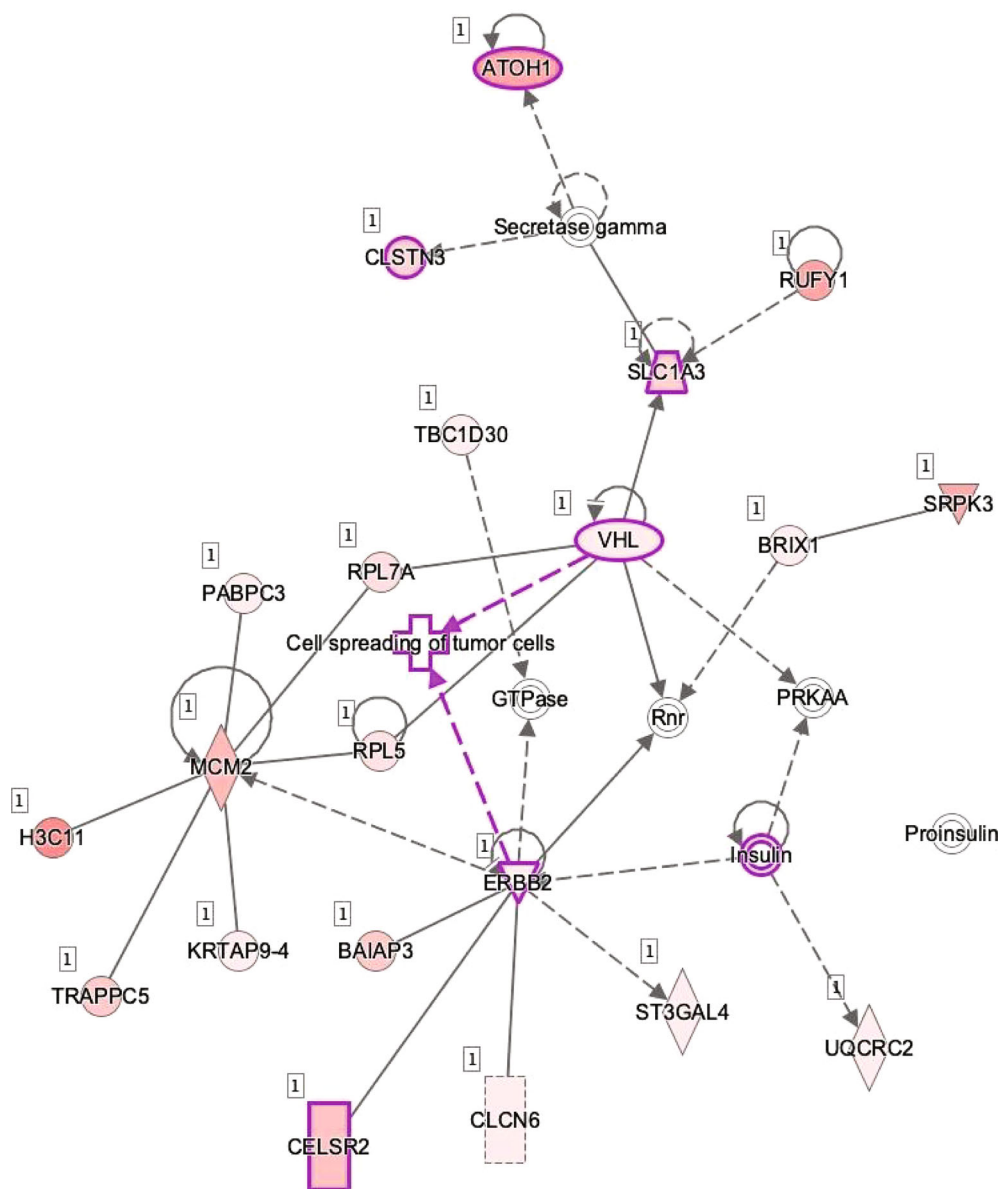


FIGURE 10: VHL gene, cell cycle, and cell morphology. This figure represents a novel regulatory network identified by IPA involving the VHL gene. Insulin as predicted to be upregulated in our dataset may be involved in the regulation of spreading of tumor cells.

2.6. *Bioinformatic and Pathway Analysis of MeDIP-Chip Results.* As before [19], *T*-tests and/or binomial tests were used to compute *p* values for differential methylation of CpG sites followed by multiple comparison correction of *p* values and computation of false detection ratio (FDR) using the Benjamini-Hochberg method [21]. Genes that are significantly differentially methylated ($p < 0.01$) between the treated vs. control groups were identified, and functional analysis of differentially methylated genes was performed using Gene Set Enrichment Analysis (GSEA). Gene promoters showing statistically significant changes in DNA methylation patterns were subjected to Ingenuity Pathway Analysis (IPA) (Ingenuity System Inc., CA, USA) for signaling pathway and gene network analysis. The *z* scores predict activation states of transcriptional regulators and were calculated by an IPA-based algorithm [19].

(http://pages.ingenuity.com/rs/ingenuity/images/0812%20upstream_regulator_analysis_whitepaper.pdf).

3. Results

3.1. *Genome-Wide Methylation Analysis and Investigation of Pathways, Functions and Networks.* The analysis of genome-wide methylation revealed that high glucose caused significant differential methylation ($p < 0.01$) in 478 gene promoters (from about -1,300 bp to +500 bp of the transcription start sites) (2.06%). There were more promoters hypomethylated (285; 1.23%) than hypermethylated (193; 0.83%) (Supplement 1a, https://docs.google.com/spreadsheets/d/10npt2_UEH9T3gX3d3qZlkm07mf5mtJf/edit#gid=1906293732).

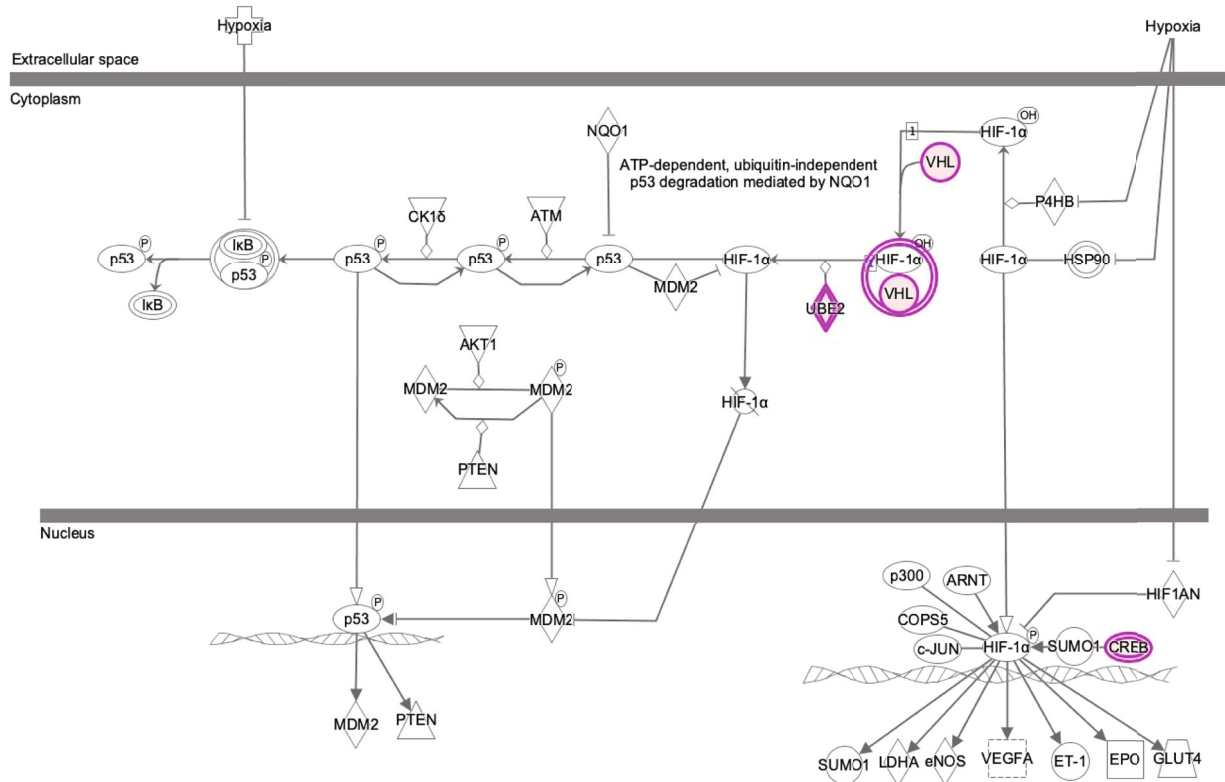


FIGURE 11: Hypoxia signaling in the cardiovascular system. This figure represents the hypoxia signaling in the cardiovascular system pathway as the main signaling pathway downregulated with a significant p value (p value = $2.13E - 02$) caused by glucose treatment.

Means for all the samples can be found in Supplement 1b (https://docs.google.com/spreadsheets/d/1_SKHu_rP3wDacDzDqUUS_zN88XaEVhUx/edit#gid=1273186519). A heat map (Figure 3) represents differential DNA methylation between treated (g1, g2, and g3) and control (C1, C2, and C3), which are grouped into two clear clusters.

As before [19], since our analysis only included significant gene promoters without intragenic and intergenic regions, we could translate our methylation data into gene expression data for IPA without complication; hypermethylated promoters are representing downregulation and hypomethylated promoters are representing upregulation of gene expression, by default [19]. We assigned positive and negative values to peak differential methylation values to correlate to upregulation or downregulation of gene expression, respectively (Supplement 2, <https://docs.google.com/spreadsheets/d/17tLE8xz3xbaNPrI9Iz18YZXOmjF4qlpt/edit#gid=407977637>). Henceforth, we will refer to these gene promoters as genes for simplicity and refer to activation from gene induction as upregulation and inhibition from gene silencing as downregulation [19].

In an initial analysis of canonical signaling pathways, biological functions, and gene networks using IPA's core analysis function, we found that significant genes were enriched in diverse canonical pathways such as the semaphorin neuronal repulsive signaling pathway (p value = $1.57E - 02$), hypoxia signaling in the cardiovascular system (p value = $2.13E - 02$), nNOS signaling in skeletal muscle cells (p value = $2.76E - 02$), the coronavirus replication pathway (p value = $2.76E - 02$),

and Rac signaling (p value = $3.24E - 02$) (Figure 4 and Figure 5). Many of these pathways are connected (Figure 6).

We particularly wanted to analyze any differential methylation caused by glucose in genes that are part of the glucose modifiers groups or involved in the etiology of DM, especially T2D. With further analysis using IPA, we linked to mechanistic networks and canonical pathways (Figure 7).

35 of these genes showed significant differential methylation (Supplement 3, https://docs.google.com/spreadsheets/d/1vV9kzpqkS4Zoc_4Hmi3lMrXrvZhpw19v/edit#gid=386233314), including CFLAR, WAS, TP73, and ERBB2.

We found many genes involved in the insulin secretion signaling pathway (Figure 8), and several genes involved in T2D signaling (Figure 9).

Furthermore, pathways are enriched in genes for molecular and cellular function, including cellular development, movement, growth, and proliferation. Novel regulatory networks involving the VHL gene, cell cycle, and cell morphology were identified (Figure 10). Metabolic reprogramming, in this case by elevated glucose, could precipitate epigenetic modifications towards cancer [22].

Therefore, a wide variety of networks and pathways were affected by an increased glucose concentration. One of the top diseases and disorders found by IPA is cancer (p value range from $1.35E - 02$ to $1.95E - 25$) with 339 molecules affected. Moreover, hypoxia signaling in the cardiovascular system pathway, including VHL, is involved (Figure 11).

We next determined the main upstream regulators, including molecules, predicted for differential regulation

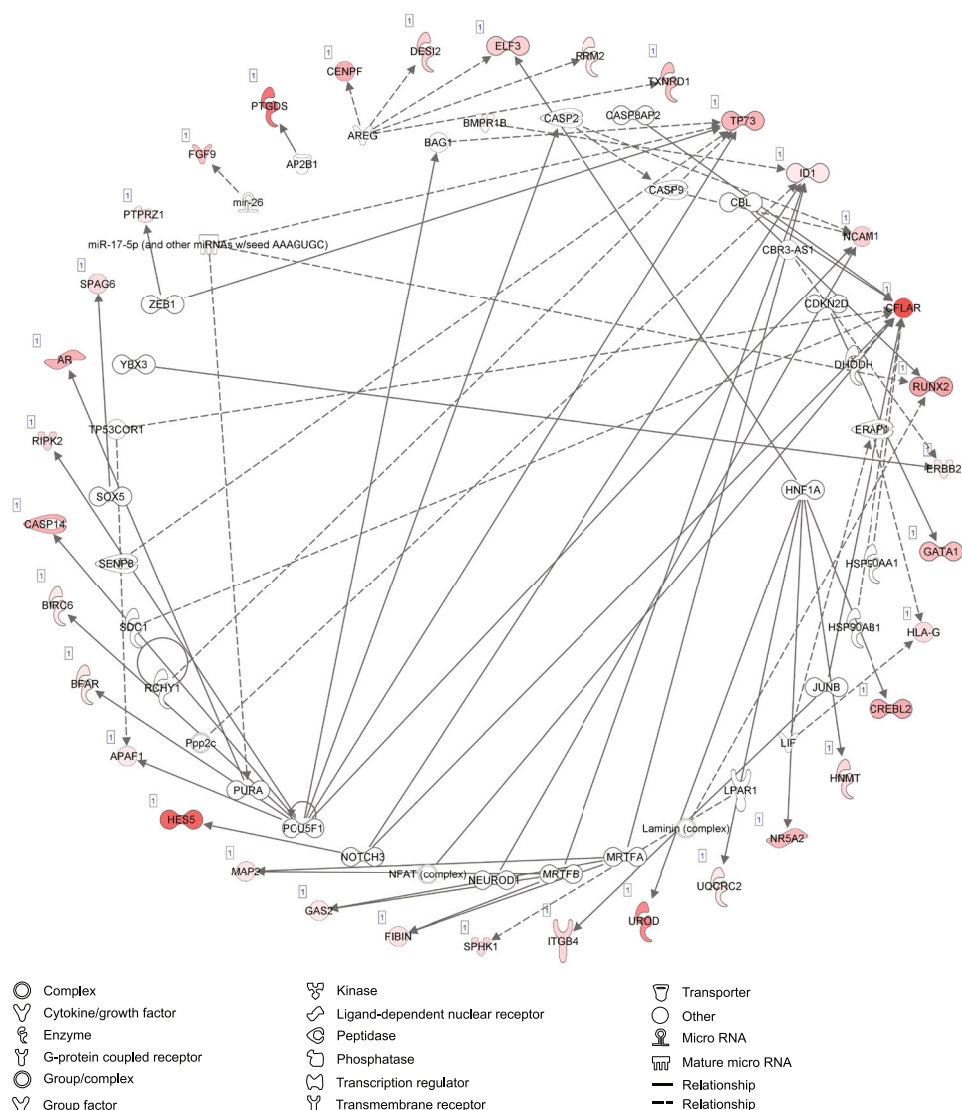


FIGURE 12: MRTFA and AREG with others identified as upstream regulators. This figure shows the many upstream regulators with predicted significant differential regulation resulting from high glucose treatment based on the hypermethylated or hypomethylated states of their downstream targets, identified by IPA upstream regulator analysis. For example, MRTFA is myocardia-related transcription factor with p value = $2.07E - 03$ and AREG is an autocrine growth factor and a mitogen for astrocytes, Schwann cells, and fibroblasts with p value = $3.24E - 03$. Other significant upstream regulators with predicted differential regulation include NOTCH3 with p value = $3.77E - 03$, POU5F1 with p value = $4.06E - 03$, and HNF1A with p value = $4.93E - 03$. As described in our previous paper [16], a dashed line means indirect interaction, a continuous line means direct interaction, a line with an arrow means “acts on”, and a line with a bar at the end means “inhibits”. The relationships between molecules represented in the figure are based on effects reported in the literature, and the color-coding in the legend is used for correlation of known relationships with observed gene expression effects resulting from glucose treatment.

based on the hypermethylated or hypomethylated state of their downstream targets (Figure 12) and found that high glucose concentration surprisingly correlated with the molecules trichostatin A (p value = $1.65E - 04$) (Figure 13) and celecoxib (p value = $2.06E - 04$) (Figure 14). This may be because trichostatin A affects the secretion pathway of beta cells and celecoxib may affect Cox-2 expression in DM.

Other significant upstream regulators with predicted differential regulation include PF-04928473 (p value = $2.11E - 04$), doxorubicin (p value = $2.37E - 04$), camptothe-

cin (p value = $2.95E - 04$), PC-SPES (p value = $6.16E - 04$), MRTFA (p value = $2.07E - 03$), AREG (p value = $3.24E - 03$), NOTCH3 (p value = $3.77E - 03$), POU5F1 (p value = $4.06E - 03$), and HNF1A (p value = $4.93E - 03$).

Out of the upstream regulators, we found five epigenetic enzymes with significant differential methylation, including DHODH, HSP90AA1, RCHY1, SDC1, and HSP90AB1 (Supplement 4, https://docs.google.com/spreadsheets/d/1AL4Rfe4s6pXee_13VtntmJOuxiPoF3N_/edit#gid=1482670607).

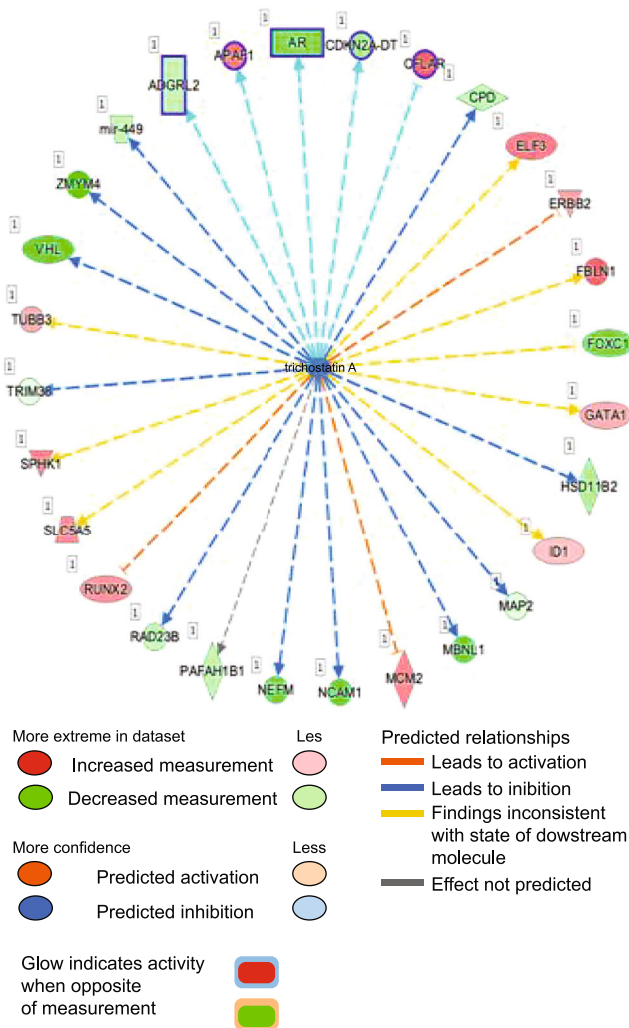


FIGURE 13: Trichostatin A. This molecule has a role in cell expression in apoptosis, acetylation, growth, transcription, activation, proliferation, binding, differentiation, and cell death. Trichostatin A is at the center, and the dotted lines with arrows indicate downstream target genes that are upregulated (red) or downregulated (green) by differential methylation as indicated in our dataset. The meaning of line and arrow style is the same as for Figure 10.

3.2. Diseases and Bio Functions. High glucose concentration impacted various cellular pathways including organismal injury and abnormalities. We identified 177 genes that were hypermethylated. Likewise, the major genes involved in these pathways are ANXA1, RPL5, HAL-G, MAP3K1, and NEDD4L. On the other hand, 379 genes were hypomethylated; for instance, SLC5A5, ID1, and SPHK1. These genes along with others were altered in (1) cellular development, growth, proliferation, and cancer; (2) gastrointestinal disease, inflammatory disease, and response; (3) cell death, survival, embryonic development, organismal injury, and abnormalities; (4) cell-to-cell signaling and interaction, hematological system development and function, and immune cell trafficking; and (5) cell cycle and ophthalmic disease (Supplement 5, <https://docs.google.com/spreadsheets/d/>

1dx1aDfZTWEsROtmGMUjnILmYDda5qmSX/edit#gid=1594460684).

In the cell death and survival network, 55 genes were linked with necrosis, apoptosis, cell survival, and viability (Figure 15).

CFLAR, ERBB2, ID1, ITGB4, OBSCN, and TP73 play a role in the cell death of breast cell lines, while APAF1, DES12, SPHK1, and miR-10 are involved in apoptosis of lung cell lines. Also, RAPGEF4 and UGCG contribute to cell death of ovarian cell lines.

These results were interesting because of the known effects of high glucose on tissue and organ development. Also, the data points to potentially new targets that can be further explored in the future.

The main physiological systems affected by high glucose included tissue development, with 5 genes involved in megakaryocytopoiesis (p value = $3.32E - 02$), 5 genes related to tubulation of vascular endothelial cells (p value = $2.18E - 02$), 4 genes related to formation of muscle (p value = $3.53E - 02$), and 3 genes related to cardiogenesis (p value = $9.89E - 03$). Additionally, cardiovascular development and function was affected, with 9 genes involved in migration of vascular endothelial cells (p value = $4.69E - 03$) and 4 genes related to permeability of endothelial cells (p value = $1.07E - 02$).

4. Discussion

We have previously outlined how epigenetics addresses the relationship between genes, environment, and disease development [5]. Epigenetic state is affected by many factors such as age, lifestyle, family history, and disease status [2]. Here, we aimed to confirm the hypothesis that epigenetic changes in pancreatic beta cells may contribute to the etiology of DM via epigenetic modifications [5]. The results show that significant epigenetic changes are induced in pancreatic beta cells by high glucose, resulting in hundreds of genes being hypomethylated or hypermethylated. Higher glucose levels can cause genome-wide DNA methylation alterations in multiple genes that are predicted to impact signaling pathways and/or physiological systems, some of which we describe as follows.

4.1. Tissue and Organ Development. In terms of the top physiological systems affected according to IPA, 47 functions related to the reproductive system and function. Androgen deficiency predisposes to metabolic syndrome and T2D in men, while conversely in women, androgen excess is predisposing [23]. Androgens regulate many aspects of cellular metabolism, protein folding, and secretion pathways. The androgen receptor (AR) is downregulated by high glucose levels. Methylation of the AR gene could lead to many diseases, e.g., cancer and developmental disorders [24]. Previous studies have confirmed androgen regulation of many genes. Many of the genes regulate signal transduction and cell cycle and play an essential role in cellular protein trafficking.

Moreover, most of them are involved in the regulation of transcription and energy metabolism. For instance, androgens have a role in promoting survival and growth of

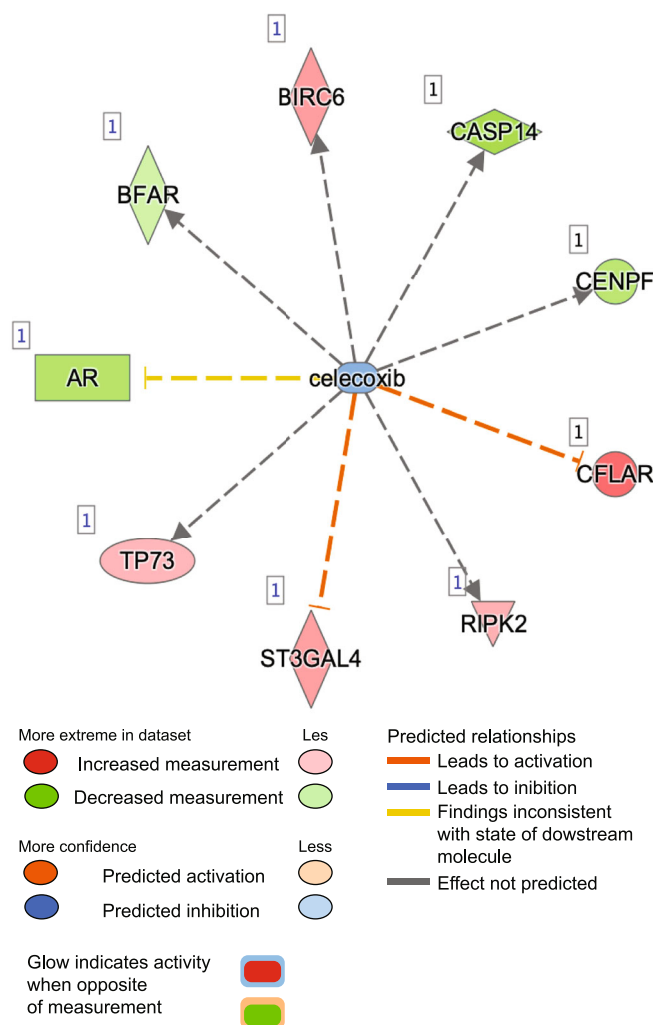


FIGURE 14: Celecoxib. This molecule has a role in cell expression in apoptosis, proliferation, growth, phosphorylation, cell death, survival, G1 phase, and activation. Celecoxib is at the center, and the dotted lines with arrows indicate downstream target genes that are upregulated (red) or downregulated (green) due to differential methylation as indicated in our dataset. The meaning of line and arrow style is the same as for Figure 10.

prostatic epithelial cells. It has also been found by a previous microarray study that androgens regulate genes related to seminal fluid production [25]. There is a bidirectional interaction between DM and androgen depletion in men; a man diagnosed with prostate cancer might develop T2D and deficiency in testosterone hormone production. Conversely, testosterone deficiency impacts the development of obesity, insulin resistance, hypogonadism, and metabolic syndrome [23]. While in women with polycystic ovary syndrome, increased testosterone levels subsequently result in impaired glucose tolerance, beta cell dysfunction, and oxidative stress [26]. These studies and ours suggest that androgen hormone alterations in T2D might be epigenetic at source and at least partly responsible for reproductive system dysfunction.

4.2. Signaling Pathways: Molecular and Metabolic Interference. Primary pathways such as sulfide oxidation IV signaling, mitochondrial L-carnitine shuttle signaling, neuronal nitric oxide synthase (nNOS) signaling in skeletal muscle cells, and hypoxia signaling in the cardiovascular system were downreg-

ulated. The sulfide oxidation pathway regulates angiogenesis, cardioprotection, cell proliferation, neural development, apoptosis, and prevention of oxidative stress [27]. Also, it participates in the relaxation of blood vessels [28]. Moreover, it plays a role in inflammatory modulation and the production of reactive oxygen species. On the other hand, accumulation of H_2S in the nervous system causes an increase in serotonin and a decrease in norepinephrine, glutamate, GABA, and aspartate [28]. nNOS signaling in skeletal muscle cells, nNOS phosphorylation, insulin stimulation, nitric oxide production, and GLUT4 translocation have all been reduced by inhibition of either nNOS or Akt2 [29].

Moreover, with a complete knockout of nNOS, in muscle strips from mice, insulin could not stimulate glucose uptake. The other signaling pathway of nNOS, when AMP-activated protein kinase (AMPK) is inhibited, prevented the activation of hydrogen peroxide (H_2O_2) and phosphorylation of nNOS, which leads to reducing NO production and significant attenuation of GLUT4 translocation [28]. Subsequently, nNOS is a common mediator of glucose uptake in both

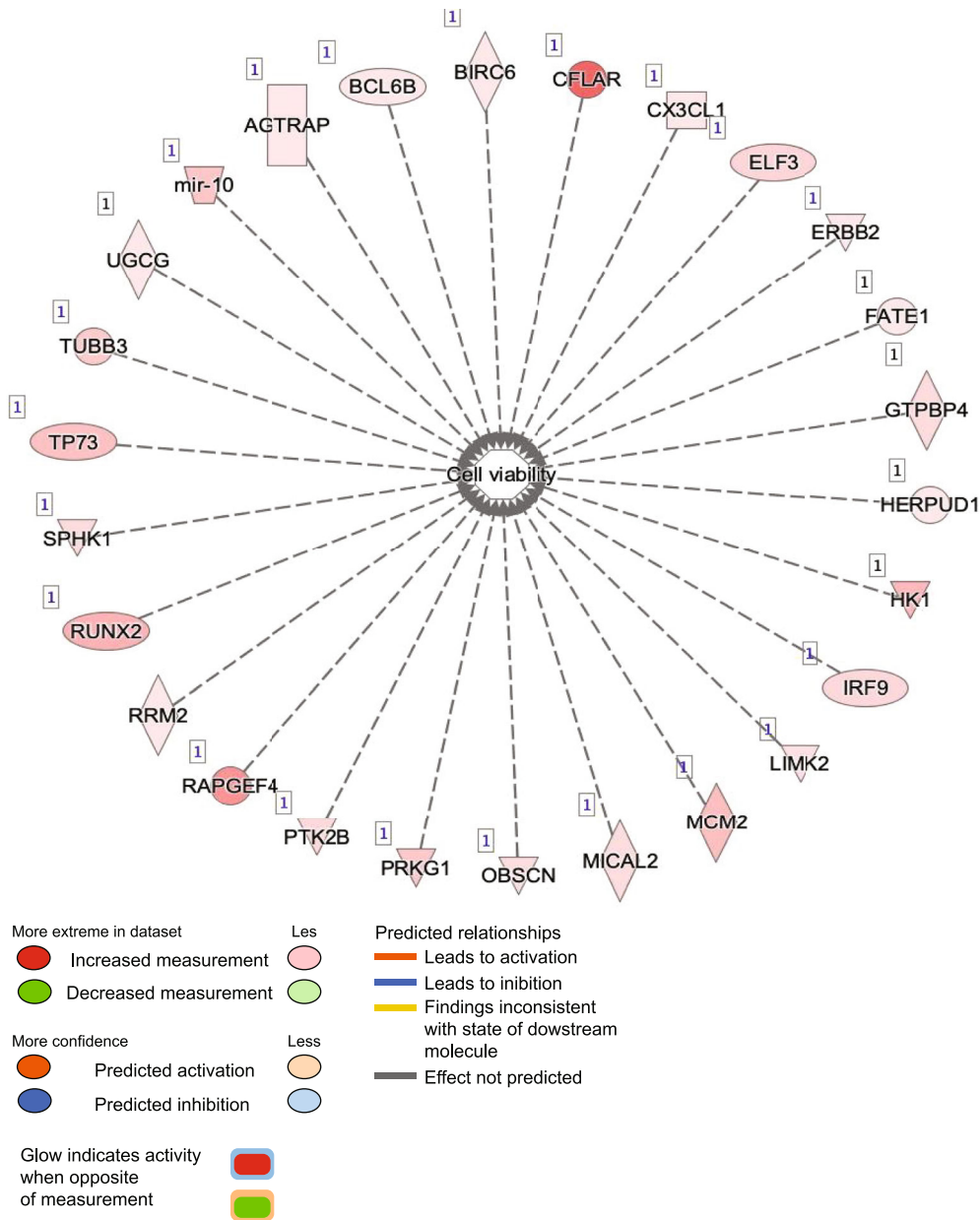


FIGURE 15: Cell viability. This figure represents many genes which may contribute to cell death and viability. Fifteen genes in the network were associated with cell death and cell survival with three of them being CFLAR, CX3CL1, and ERBB2 which were associated with survival of microglia network.

pathways, so the activation of both insulin and H₂O₂ signaling pathways will converge on nNOS [29].

Mitochondrial function is needed to produce ATP, and mitochondria are critical regulators of glucose to stimulate insulin secretion. During the past two decades, it has been found that mitochondrial dysfunction impacts DM, especially T2D, and involves many mechanisms, such as obesity, insulin resistance, pancreatic β -cell dysfunction, and vascular complications [30]. Another interesting finding in the data is the involvement of pathways for hypoxia signaling in the cardiovascular system. It will be important to integrate the role of hypoxia-inducible factors in DM with epigenetics [31].

4.3. Apoptosis and Death Receptors. Many studies suggest that endothelial damage and dysfunction is one of the early steps in the development of vascular complications. There is a close correlation between hyperglycemia and abnormalities in endothelial function and morphology [32]. Furthermore, high glucose levels increase DNA damage, affect the cell cycle, delay endothelial cell replication, and cause cell death in cultured human endothelial cells. Also, cell death of retinal microvascular cells leads to diabetic retinopathy. Apoptosis in mammals may be initiated by two different pathways that ultimately converge into a common pathway, resulting in effector enzyme caspase activation [32]. We identified four genes from the upstream regulators belonging

to the caspase family of proteins: CASP2, CASP9, and CASP14, which are peptidases, and CASP8AP2, which is a transcription regulator associated with cell death survival, all differentially methylated by high glucose. Recent studies have shown that high glucose causes decreased mitochondrial membrane potential and the release of cytochrome c in human umbilical vein endothelial cells. Also in high glucose, gene expression levels of the death receptors TNF-R1 and Fas were increased [32]. Activation of caspases ultimately leads to cell disintegration [33].

4.4. Oxidative Stress. Oxidative stress affects cellular metabolism. Endoplasmic reticulum (ER) stress occurs when proteins are misfolded during biosynthesis. As a result of the unfolded protein response in beta cells, insulin transcription and translation are reduced, and inflammation and apoptosis initiated, while protein misfolding causes the production of reactive oxygen species (ROS) [34, 35]. Thus, beta cell dysfunction involving oxidative and ER stress, impaired secretory function, beta cell apoptosis, and islet inflammation might progressively cause T2D. Accumulation of β -amyloid, which is one feature of human diabetic islets, has been connected to oxidative stress and apoptosis without ER stress [34, 35]. We found one gene, SUOX, with significant methylation (p value = $2.04E - 03$) that has a role in oxidoreductase activity, protein binding, and sulfite oxidase activity. Oxidative stress is considered a crucial feature of beta cell dysfunction in T2D and of beta cell depletion in type 1 diabetes. Also, oxidative stress has many harmful effects on beta cell function, including suppression of insulin transcription. However, some ROS production is needed for signaling within beta cells and normal beta cell function [34, 35].

4.5. Study Limitations. Finally, there are some limitations with this study. Firstly, only beta cells were used in the experiment, but *in vivo*, pancreatic islets contain other cells -alpha and others- which could affect the cells' behavior *in vivo*. Secondly, we have not yet looked at reversibility of the epigenetic changes, and it is possible that some of these changes are reversible if the glucose level is normalized. This will be the focus of future experiments. Lastly, *in vivo* glucose levels fluctuate, but in our study, they were constant and unchanging. We will try to replicate more "lifelike" glucose fluctuations in future experiments.

5. Conclusions

In this study, we wanted to explore the potential of high glucose levels to cause epigenetic changes in human beta cells in an initial trial experiment. We used human genome-wide promoter methylation analysis to identify alterations caused by a high glucose concentration. MeDIP-Chip microarray analysis revealed that many genes were hypermethylated or hypomethylated. We have highlighted canonical pathways and mechanistic networks that are related to DM. The networks that were found as a result of this analysis may provide insight into genes that can be further studied. They may provide valuable knowledge pointing to epigenetic changes in pancreatic beta cells in the etiology of DM. We

view this paper as the beginning of a more extensive investigation into the epigenetic mechanisms and potential etiology of DM.

A future investigation will also include metformin. Metformin might change the epigenetic networks at least partially back to normal and influence and stimulate beta cells to increase insulin hormone secretion. It will be important to explore this hypothesis further in future studies: to better understand the epigenetic changes in pancreatic beta cells in DM and also understand their reversibility.

Data Availability

Supplementary files are available on Google Drive at: <https://drive.google.com/drive/u/0/folders/1J80zzwrZb6S7CgHVvzkIXR-Av6lj-Inf>.

Disclosure

The content is solely the responsibility of the authors and does not necessarily represent the official views of the NIH.

Conflicts of Interest

The authors declare that there are no conflicts of interest regarding the publication of this manuscript.

Acknowledgments

We thank Dr. William Southerland and RCMI at Howard University for providing us access to IPA Software. This research was supported by the National Institutes of Health (NIH) R25 Resource Grant (1 R25 AG047843-01) to ABC and by the National Science Foundation (NSF IOS-1355034), Howard University College of Medicine, and the District of Columbia Center for AIDS Research, an NIH-funded program (P30AI117970), to TH. This program is supported by the following NIH cofunding and participating institutes and centers: NIAID, NCI, NICHD, NHLBI, NIDA, NIMH, NIA, NIDDK, NIMHD, NIDCR, NINR, FIC, and OAR.

Supplementary Materials

Supplement 1a: data was processed following the protocol of our previous paper [16]. Table with a list of significantly differentially methylated peaks ($p < 0.01$) that lie within 2000 base pairs of the transcription start site of a gene, generated using the initial raw data. All coordinates were transformed from hg18 to hg38, and the genes were reannotated. Peaks were remapped to the latest genome (hg38) and refiltered according to distance from the nearest gene TSS. The "Direction" column indicates which way the differential methylation goes (hypermethylated in treated or hypomethylated). The "Peak differential methylation" column (col M) shows the average difference in methylation level between treated and untreated (positive values are higher methylation in treated compared to untreated; negatives are lower). There are more peaks hypomethylated in treated than hypermethylated (285 hypomethylated peaks vs. 193

hypermethylated peaks). Each peak lies within 2000 base pairs of one or more genes. The list of genes is in column C and the distance of their TSS from the middle of the peak is in column L. Positive numbers indicate that the peak middle is upstream of the TSS, and negative numbers indicate that the peak middle is downstream. Supplement 1b: means for all of the significant peaks. Supplement 2: data was processed following the protocol of our previous paper [16]. Table with list of significantly differentially methylated peaks ($p < 0.01$) that lie within 2000 base pairs of the transcription start site of a gene, used as raw data for IPA. Hypomethylated gene promoters with significantly differentially methylated peaks were assigned positive signs, and hypermethylated gene promoters were assigned negative signs, to correlate with upregulation or downregulation of gene expression, respectively. Supplement 3: data was processed following the protocol of our previous paper [16]. Table listing all genes linked to mechanistic networks and canonical pathways. Information regarding gene/molecule and their respective ENTREZ Gene IDs for human, mouse, and rat are specified. Supplement 4: data was processed following the protocol of our previous paper [16]. Table listing significant upstream regulators with predicted differential regulation. From these upstream regulator's gene, five epigenetic enzymes were found with significant differential methylation. Supplement 5: data was processed following the protocol of our previous paper [16]. An all-inclusive list of organismal injury and abnormalities-related genes based on significant genes from our dataset as identified by IPA analysis of high glucose treated human cells. Each function with p value and activation z score, genes/molecule names, and total number of genes/molecules with predicted differential regulation from high glucose treatment are listed. (*Supplementary Materials*)

References

- [1] J. K. Wolford and B. Vozarova de Courten, "Genetic basis of type 2 diabetes mellitus," *Treatments in Endocrinology*, vol. 3, no. 4, pp. 257–267, 2004.
- [2] R. R. Kanherkar, N. Bhatia-Dey, and A. B. Csoka, "Epigenetics across the human lifespan," *Frontiers in Cell and Development Biology*, vol. 2, p. 49, 2014.
- [3] A. B. Csoka and M. Szyf, "Epigenetic side-effects of common pharmaceuticals: a potential new field in medicine and pharmacology," *Medical Hypotheses*, vol. 73, no. 5, pp. 770–780, 2009.
- [4] R. R. Kanherkar, S. E. Stair, N. Bhatia-Dey, P. J. Mills, D. Chopra, and A. B. Csoka, "Epigenetic mechanisms of integrative medicine," *Evidence-based Complementary and Alternative Medicine*, vol. 2017, Article ID 4365429, 19 pages, 2017.
- [5] R. A. Alhazzaa, T. Heinbockel, and A. B. Csoka, "Diabetes and epigenetics," in *Epigenetics to Optogenetics - a New Paradigm in the Study of Biology*, M. Anwar, Z. Farooq, R. A. Rather, M. Tauseef, and T. Heinbockel, Eds., IntechOpen, London, 2022.
- [6] L. M. Villeneuve and R. Natarajan, "The role of epigenetics in the pathology of diabetic complications," *American Journal of Physiology-Renal Physiology*, vol. 299, no. 1, pp. F14–F25, 2010.
- [7] E. Nilsson and C. Ling, "DNA methylation links genetics, fetal environment, and an unhealthy lifestyle to the development of type 2 diabetes," *Clinical Epigenetics*, vol. 9, no. 1, p. 105, 2017.
- [8] T. Dayeh and C. Ling, "Does epigenetic dysregulation of pancreatic islets contribute to impaired insulin secretion and type 2 diabetes?," *Biochemistry and Cell Biology*, vol. 93, no. 5, pp. 511–521, 2015.
- [9] D. Bernstein, M. L. Golson, and K. H. Kaestner, "Epigenetic control of β -cell function and failure," *Diabetes Research and Clinical Practice*, vol. 123, pp. 24–36, 2017.
- [10] A. Moosavi and A. Motevalzadeh Ardekani, "Role of epigenetics in biology and human diseases," *Iranian Biomedical Journal*, vol. 20, no. 5, pp. 246–258, 2016.
- [11] J. Liang, S. Y. Wu, D. Zhang, L. Wang, K. K. Leung, and P. S. Leung, "NADPH oxidase-dependent reactive oxygen species stimulate β -cell regeneration through differentiation of endocrine progenitors in murine pancreas," *Antioxidants & Redox Signaling*, vol. 24, no. 8, pp. 419–433, 2016.
- [12] M. Heinis, M. T. Simon, K. Ilc et al., "Oxygen tension regulates pancreatic β -cell differentiation through hypoxia-inducible factor 1 α ," *Diabetes*, vol. 59, no. 3, pp. 662–669, 2010.
- [13] M. Heinis, A. Soggia, C. Bechetoille et al., "HIF1 α and pancreatic β -cell development," *FASEB Journal*, vol. 26, no. 7, pp. 2734–2742, 2012.
- [14] B. Sun, X. H. Meng, R. Liu, S. Yan, and Z. D. Xiao, "Mechanism study for hypoxia induced differentiation of insulin-producing cells from umbilical cord blood-derived mesenchymal stem cells," *Biochemical and Biophysical Research Communications*, vol. 466, no. 3, pp. 444–449, 2015.
- [15] C. Chen, C. M. Cohrs, J. Stertmann, R. Bozsak, and S. Speier, "Human beta cell mass and function in diabetes: recent advances in knowledge and technologies to understand disease pathogenesis," *Molecular Metabolism*, vol. 6, no. 9, pp. 943–957, 2017.
- [16] N. Ma and E. Mm, "Antidiabetic and antioxidative potential of *Cystoseira myrica*," *American Journal of Biochemistry*, vol. 4, pp. 59–67, 2014.
- [17] A. Ahangarpour, F. R. Ali Akbari, and H. F. Moghadam, "Effect of C-peptide alone or in combination with nicotinamide on insulin levels from pancreatic islets in mouse," *The Malaysian Journal of Medical Sciences*, vol. 23, no. 1, pp. 15–21, 2016.
- [18] R. P. Robertson, J. Harmon, P. O. Tran, Y. Tanaka, and H. Takahashi, "Glucose toxicity in β -cells: type 2 diabetes, good radicals gone bad, and the glutathione connection," *Diabetes*, vol. 52, no. 3, pp. 581–587, 2003.
- [19] R. R. Kanherkar, B. Getachew, J. Ben-Sheetrit et al., "The effect of citalopram on genome-wide DNA methylation of human cells," *International Journal of Genomics*, vol. 2018, Article ID 8929057, 25 pages, 2018.
- [20] K. D. Siegmund, "Statistical approaches for the analysis of DNA methylation microarray data," *Human Genetics*, vol. 129, no. 6, pp. 585–595, 2011.
- [21] Y. Benjamini, D. Drai, G. Elmer, N. Kafkafi, and I. Golani, "Controlling the false discovery rate in behavior genetics research," *Behavioural Brain Research*, vol. 125, no. 1–2, pp. 279–284, 2001.
- [22] L. Sun, H. Zhang, and P. Gao, "Metabolic reprogramming and epigenetic modifications on the path to cancer," *Protein & Cell*, vol. 13, no. 12, pp. 877–919, 2022.

- [23] G. Navarro, C. Allard, W. Xu, and F. Mauvais-Jarvis, "The role of androgens in metabolism, obesity, and diabetes in males and females," *Obesity*, vol. 23, no. 4, pp. 713–719, 2015.
- [24] H.-J. Jin, J. Kim, and J. Yu, "Androgen receptor genomic regulation," *Translational Andrology and Urology*, vol. 2, pp. 158–177, 2013.
- [25] S. E. DePrimo, M. Diehn, J. B. Nelson et al., "Transcriptional programs activated by exposure of human prostate cancer cells to androgen," *Genome Biology*, vol. 3, no. 7, article RESEARCH0032, 2002.
- [26] E. Diamanti-Kandarakis and A. Dunaif, "Insulin resistance and the polycystic ovary syndrome revisited: an update on mechanisms and implications," *Endocrine Reviews*, vol. 33, no. 6, pp. 981–1030, 2012.
- [27] F. Bouillaud and F. Blachier, "Mitochondria and sulfide: a very old story of poisoning, feeding, and signaling?," *Antioxidants & Redox Signaling*, vol. 15, no. 2, pp. 379–391, 2011.
- [28] C. M. Quinzii, M. Luna-Sanchez, M. Ziosi, A. Hidalgo-Gutierrez, G. Kleiner, and L. C. Lopez, "The Role of Sulfide Oxidation Impairment in the Pathogenesis of Primary CoQ Deficiency," *Frontiers in Physiology*, vol. 8, p. 525, 2017.
- [29] D. L. Kellogg, K. M. McCammon, K. S. Hinchee-Rodriguez, M. L. Adamo, and L. J. Roman, "Neuronal nitric oxide synthase mediates insulin- and oxidative stress-induced glucose uptake in skeletal muscle myotubes," *Free Radical Biology & Medicine*, vol. 110, pp. 261–269, 2017.
- [30] S. H. Kwak, K. S. Park, K. Lee, and H. K. Lee, "Mitochondrial metabolism and diabetes," *Journal of Diabetes Investigation*, vol. 1, no. 5, pp. 161–169, 2010.
- [31] D. Pirri, M. Fragiadaki, and P. C. Evans, "Diabetic atherosclerosis: is there a role for the hypoxia-inducible factors?," *Bioscience Reports*, vol. 40, no. 8, p. BSR20200026, 2020.
- [32] S. Kageyama, H. Yokoo, K. Tomita et al., "High glucose-induced apoptosis in human coronary artery endothelial cells involves up-regulation of death receptors," *Cardiovascular Diabetology*, vol. 10, no. 1, p. 73, 2011.
- [33] A. B. Parrish, C. D. Freel, and S. Kornbluth, "Cellular mechanisms controlling caspase activation and function," *Cold Spring Harbor Perspectives in Biology*, vol. 5, no. 6, article a008672, 2013.
- [34] S. Z. Hasnain, J. B. Prins, and M. A. McGuckin, "Oxidative and endoplasmic reticulum stress in β -cell dysfunction in diabetes," *Journal of Molecular Endocrinology*, vol. 56, no. 2, pp. R33–R54, 2016.
- [35] D. M. Muoio and C. B. Newgard, "Molecular and metabolic mechanisms of insulin resistance and β -cell failure in type 2 diabetes," *Nature Reviews Molecular Cell Biology*, vol. 9, no. 3, pp. 193–205, 2008.

Research Article

Oxidative and Cellular Stress Markers in Postmenopause Women with Diabetes: The Impact of Years of Menopause

Carolain Felipin Vincensi Anklam,^{1,2} Yana Picinin Sandri Lissarassa,^{1,2} Analú Bender dos Santos,^{1,2} Lílian Corrêa Costa-Beber,^{1,2} Lucas Machado Sulzbacher,^{1,2} Pauline Brendler Goettens-Fiorin,^{1,2} Thiago Gomes Heck ,^{1,2,3} Matias Nunes Frizzo,^{1,2} and Mirna Stela Ludwig ^{1,2}

¹Research Group in Physiology, Department of Life Sciences, Regional University of Northwestern Rio Grande Do Sul State (UNIJUI), Rua do Comércio, 3000 Bairro Universitário Ijuí RS, Brazil 98700-000

²Postgraduate Program in Integral Attention to Health (PPGAIS-UNIJUI/UNICRUZ), Ijuí, RS, Brazil

³Postgraduate Program in Mathematical and Computational Modeling (PPGMMC-UNIJUI), Ijuí, RS, Brazil

Correspondence should be addressed to Thiago Gomes Heck; thiago.heck@unijui.edu.br and Mirna Stela Ludwig; ludwig@unijui.edu.br

Received 26 May 2021; Accepted 28 August 2021; Published 16 September 2021

Academic Editor: Andrea Scaramuzza

Copyright © 2021 Carolain Felipin Vincensi Anklam et al. This is an open access article distributed under the Creative Commons Attribution License, which permits unrestricted use, distribution, and reproduction in any medium, provided the original work is properly cited.

Women live approximately one-third of their lives in postmenopause. Among postmenopausal women, type 2 diabetes mellitus (DM2) is one of the most prevalent chronic diseases. These conditions promote alterations in the oxidative, metabolic, and immune-inflammatory profiles marked by higher extracellular 72 kDa-heat shock protein (eHSP72). Here, we investigated whether the time of menopause is associated with oxidative cellular stress marker levels in postmenopausal women with DM2. Sixty-four women were recruited (56.7 ± 12.6 years old) in the pre- ($n = 22$) and postmenopause ($n = 42$) period, with ($n = 19$) or without DM2 ($n = 45$), and a fasting blood collection was made for the evaluation of metabolic, oxidative, and inflammatory markers. We found that menopause and DM2 influenced metabolic and oxidative parameters and presented synergistic effects on the plasma lipoperoxidation levels. Also, postmenopausal women had the highest eHSP72 concentration levels associated with the years in postmenopause. We conclude that the time of menopause impacts the markers of cellular stress and increases the risk of oxidative stress, mainly when it is associated with DM2.

1. Introduction

Population aging observed in most countries has led women to live one-third of their lives in the postmenopausal condition [1]. Menopause marks the end of the reproductive life and is characterized by the decline of 17β -estradiol levels. It predisposes to oxidative stress [2], vasomotor symptoms [3], osteoporosis, and chronic diseases, such as obesity and type II diabetes mellitus (DM2) [4].

DM2 is one of the most prevalent chronic diseases in postmenopausal women and is characterized by metabolic disorders, as well as a chronic low-grade inflammatory and oxidative disbalance. Oxidative stress appears to be central

in the DM2 progression since the lipoperoxidation increases according to the disease severity [5]. Hence, the global (metabolic, oxidative, and inflammatory) impairment that characterizes DM2 can increase the susceptibility to complications when associated with low estrogen levels [6].

Both DM2 and hypoestrogenism imply changes in the cellular stress response, mainly the 72 kDa-heat shock proteins (HSP72) [7]. The anti-inflammatory, antiapoptotic, and cytoprotective roles of HSP72 in the intracellular medium contrast with its effects in the extracellular medium [8]. HSP72 is released to the extracellular milieu (eHSP72), and, when circulating, it can bind to toll-like receptors and act in the proinflammatory and damage signaling [9].

Therefore, managing its plasmatic concentration may represent a potential therapeutic target [10, 11].

It was previously reported that the circulating levels of HSP72 are associated with cardiovascular risk in postmenopausal women with diabetes [12]. In this sense, the role of eHSP72 as predictive in clinical conditions [10, 11], mainly chronic and inflammatory ones, has been investigated [13]. Hence, the eHSP72 plasmatic concentration along the postmenopausal period could help identify the physiopathological relationships between postmenopause and DM2. However, whether it is sensitive to the low-grade inflammation that marks postmenopause plus DM2 and the follow-up of this scenario years after menopause remains unclear. Thus, we hereby evaluated if the time of postmenopause affects the circulating levels of eHSP72 in diabetic women and if it is associated with an oxidative and inflammatory profile.

2. Methods

Women participating in care groups in the Family Health Strategies of a town in southern Brazil were recruited and participated in our study. Initially, 73 women were administered face-to-face interviews to obtain sociodemographic information, medical history of chronic diseases, time of amenorrhea, use of medications, and dietary survey. Further, we applied as exclusion criteria the current use of hormonal replacement therapy, cancer, autoimmune, acute infection, nontreated hypertension, smoking, undergoing chemotherapy treatment, and the regular or eventual use of insulin. We ended up with 64 women participating in our study. The calculation of the sample number was done based on the expected difference for the most important variable in this study, the circulating concentration of eHSP72, as in the Nakhjavani et al. [14] study, and indicates a number of 15 subjects per group. We used a statistical power of 95%, with a significance level of 0.05%. It is worth noting that, during the study, the number of samples used for each parameter varied (as expressed in the figure and table legends) due to its technical conditions for the analysis.

The participants were initially divided in two groups: premenopause ($n = 22$) and postmenopause ($n = 42$). Postmenopause was defined as amenorrhea of 12 months, at least, which was confirmed by the estrogen (17β -estradiol) levels (premenopause: 55.3 ± 54.7 pg/mL and postmenopause 25.3 ± 18.6 pg/mL). Finally, they were divided in subgroups: premenopause without DM2 ($n = 15$), premenopause with DM2 ($n = 7$), postmenopause without DM2 ($n = 30$), and postmenopause with DM2 ($n = 12$), based on medical diagnosis of DM2 or by fasting glycemia ≥ 126 mg/dL and HbA1c $> 6.5\%$ [15]. Based on Nakhjavani et al.'s [14] study, which showed that long-standing diabetes had higher eHSP72 levels than controls, we expect similar biological evidence (difference of eHSP72 levels $\sim 0.58 \pm 0.35$ ng/mL) to reach a statistical power of 95%, with a significance level of 0.05% when comparing premenopause without DM2 vs. postmenopause with DM2. The study had 95.0% power to detect an effect size of 0.509 using T statis-

tics or better (0.489) using the Z statistic instead of the T statistics.

The study was made in agreement with the Regulatory Guidelines and Norms for Research Involving Humans, according to Resolution of the National Health Council (CNS) n°. 466/2012 and was approved by the Ethics Committee (n° 1.173.158).

2.1. Anthropometric Analyses. Bodyweight (kg) was verified using a calibrated scale and the height (cm) and waist circumference (WC), abdominal (AC), and hip circumference (HC), with a standard measuring tape. To analyze WC, we admitted the Brazilian Guidelines of Obesity 2009-2010 and its values of risk for metabolic complications [16]. We also evaluated the waist-to-hip ratio by the direct quotient between waist and hip circumference, classified according to the cut points recommended by World Health Organization [16].

We calculated body mass index (BMI) using the Quetelet equation, $BMI (kg/m^2) = mass (kg)/height (m)^2$ and analyzed it according to the Brazilian Association for the Study of Obesity guidelines [16]. As a complement, we evaluated the adiposity index using the equation $Adiposity Index = [HC (cm)/height (m) \times \sqrt{height (m)}] - 18$ [17] and the conicity index according to the formula $Conicity Index = WC (m)/0.109 \times \sqrt{weight (kg)/height (m)}$.

2.2. Blood Collection. Biochemical analyses were performed in blood collected from patients after 10 to 12 hours of fasting. Blood was immediately separated in vacuum tubes with and without ethylenediaminetetraacetic acid (EDTA). Blood with EDTA was used for total blood aliquot and plasma separation. Blood without EDTA was used to obtain serum. Aliquots for plasma and serum were centrifuged for 30 minutes at 3.000 rpm. Total blood was used to measure glycated hemoglobin, erythrocyte sedimentation rate, and leukometry; serum was used to measure E2 levels as well as lipid, glycemic, and hepatic profiles. Plasma samples were frozen in liquid nitrogen with phenyl methyl sulfonyl fluoride (PMSF, Sigma P7626, FW = 174.19 g/mol) ($1.74 \text{ mg/mL} = 100 \text{ mM}$) for subsequent measurement of malondialdehyde (MDA) and eHSP72 levels.

2.3. Dosage of 17β Estradiol. A quantitative dosage of 17β -estradiol (E2) was performed in a serum sample through the automated system ADVIA Centaur XP (Siemens Healthcare Diagnosis) by chemiluminescence methodology with sensitivity and in vitro test limits higher than 20 pg/mL. The results were expressed in pg/mL.

2.4. Lipid, Glycemic, and Hepatic Profile. Total cholesterol, HDL, triglycerides levels, and fasting glycemia were analyzed in serum samples by an enzymatic-colorimetric method using Bioclin-Quibasa kits in BS200-Mindray automation. LDL was indirectly verified by the Friedewald equation $LDL = CT - HDL - TG/5$, where TG/5 represents the cholesterol bound to VLDL-C [18].

Glycated hemoglobin was measured in total blood aliquot by high-performance liquid chromatography (HPLC)

and expressed in percentage. The mean glycemia was estimated by the formula (Mean glycemia = $28.7 \times \text{HbA1C}$) – 46.7, in agreement with the recommendations from the Brazilian Society of Diabetes [15]. All other results were expressed in mg/dL.

Hepatic enzymes were measured in serum samples. Alkaline phosphatase (ALP), glutamic-oxaloacetic transaminase (GOT), glutamic-pyruvic transaminase (GPT), and gamma-glutamyl transferase (GGT) were measured by kinetic methods using Biclin-Quibasa kits. The results were expressed in U/L.

2.5. Inflammatory Status. Ultrasensitive C-reactive protein was measured in serum samples by turbidimetry. The results were expressed in mg/dL. Erythrocyte sedimentation rate was verified in total blood by Westergren's pipette technique. Leukometry was measured by impedance counting, obtaining the number of total leukocytes/mm³.

eHSP72 levels were verified in plasma samples by a highly sensitive enzyme-linked immunosorbent assay. We used an HSPA1A-specific HSP72 ELISA Kit (ENZO Life Sciences, ENZ-KIT-101) according to the manufacturer's recommendations. A standard curve was constructed from known dilutions of HSP72 recombinant protein to allow a quantitative assessment of eHSP72 plasma concentration. Quantification was done using a microplate reader (Mindray MR-96A) at 450 nm, and the intra-assay coefficient of variation was identified as being <2%. Results were expressed in ng/mL.

2.6. Lipoperoxidation. Lipoperoxidation was measured by the MDA levels using the thiobarbituric acid reactive substances method (TBARS) [19]. Briefly, 25 μL of plasma was incubated with 20 μL water, 125 μL thiobarbituric acid (TBA, 0.6%), 5 μL butylated hydroxytoluene (BHT, 10 mM), 300 μL of phosphoric acid (H_3PO_4 , 1%), and 25 μL sodium dodecyl sulfate (SDS, 8.1%) for 60 min at 100°C. After this, tubes were centrifuged, the supernatant collected, and the absorbance verified in a plate reader (DR-200BS model, Kasuaki, PR, Brazil) at 505 nm. The MDA standard was prepared from 1.1.3.3-Tetramethoxypropane (points from 0.0005–0.016 mg/mL). Results were expressed in mmol MDA/mg of protein.

2.7. Statistical Analysis. Initially, we verified the data normality by the Kolmogorov-Smirnoff test. We compared means of E2 and eHSP72 levels between pre- and postmenopausal women using the Student's *t*-test and evaluated the association between menopause and eHSP72 levels by chi-square test.

We further distributed women in groups according to the "time of menopause" and "age" based on the median values of time of postmenopause and age (expressed in years). We compared eHSP72, CRP, and E2 levels between the established groups using one-way ANOVA, followed by Tukey. We also evaluated the effect of interaction between DM2 and menopause in different parameters by using two-way ANOVA, followed by Tukey.

For analyses of the association between anthropometric, metabolic parameters, time of menopause, presence of DM2, and time of DM2 with the eHSP72 levels (dependent variable), we used the univariate and multivariate regression and the Pearson correlation. We adjusted the quadratic regression to be linear.

The data were processed by Graphpad Prism 9.0, and the results were expressed in mean \pm standard deviation.

3. Results

The mean age of the 64 women was 56.7 ± 12.6 years. The premenopausal women ($n = 22$) presented 43.3 ± 8.0 years and the postmenopausal women ($n = 42$), 63.5 ± 8.3 years. The mean value of abdominal circumference (AC) was higher than 88 cm (value indicating metabolic risk) in all groups, reaching 94% of postmenopausal women and 86% of premenopausal women. About 30% of the women were included in the DM2 group. Of these women, 63% reported hot flushes compared to 42% of the postmenopausal without DM2. Among postmenopausal women, 88% (37) reported using statins and presented LDL levels below 150 mg/dL.

As expected, the fasting glycemia, HbA1c, and MEG were higher for diabetic women, without differing for pre- and postmenopausal women.

LDL was influenced by both risk factors, isolated or associated (Table 1). Postmenopausal women with DM2 presented a lower concentration of LDL compared to postmenopausal women without DM2 (Table 1), and these values were inversely related to the use of statins. DM2 also enhanced triglycerides levels, and this effect was similar between pre- and postmenopausal women. Total cholesterol was influenced by diabetes, without an additional effect of menopause (Table 1).

In general, the hepatic profile was also disturbed by menopause and DM2. The serum levels of GGT were enhanced by the interaction between factors. Premenopausal women with diabetes presented higher levels of GGT than all other groups. In addition, postmenopausal women with diabetes presented higher GGT levels than postmenopausal women without diabetes. The ALP was affected by menopause, and the effect was similar in women with or without DM2. The transaminases were not responsive to the factors (Table 1).

Further, we verified the lipoperoxidation in the plasma by evaluating the MDA levels, and we found that it was influenced by both factors, isolated or associated. Postmenopausal women with DM2 presented higher levels of MDA compared to premenopausal women with or without DM2, as well as compared to postmenopausal women with DM2 (Table 1). Thus, we performed multivariate regression analysis between the MDA levels (independent variable) and the menopause status, women's age, and DM2 diagnosis, and the statistics confirmed an association between MDA levels and DM2 diagnosis ($R^2_{aj} = 0.27$; $p = 0.0009$).

The leukometry analysis showed an influence of menopause and the interaction between both risk factors in a way that postmenopausal women with DM2 presented more leukocytes compared to postmenopausal women without DM2. The erythrocyte sedimentation rate (ESR) was also

TABLE 1: Anthropometric, metabolic, oxidative, inflammatory, and hepatic parameters from pre- and postmenopausal women, with or without DM2 diagnosis.

Parameters		Premenopausal	Premenopausal with DM2	Postmenopausal	Postmenopausal with DM2	<i>p</i> value
Anthropometric parameters	BMI	30.42 ± 4.46	33.94 ± 8.26	31.02 ± 4.96	28.67 ± 6.02	n/s
	AC	101.13 ± 10.31	101.00 ± 14.75	101.90 ± 8.01	95.17 ± 10.87	n/s
	WHR	0.87 ± 0.09	0.92 ± 0.05	0.92 ± 0.06	0.92 ± 0.06	n/s
	BAI	35.48 ± 3.45	39.60 ± 10.90	37.70 ± 5.05	35.27 ± 4.55	n/s
	CI	1.24 ± 0.12	1.30 ± 0.08	1.32 ± 0.08	1.32 ± 0.11	n/s
Metabolic parameters	Gli	92.00 ± 7.58	132.86 ± 25.94 _{ab}	92.47 ± 8.03	136.92 ± 31.40 ^{ab}	Menopause <i>p</i> = 0.6450, diabetes <i>p</i> < 0.0001, interaction <i>p</i> = 0.7144
	HbA1c	5.40 ± 0.33	6.80 ± 1.10 ^{ab}	5.85 ± 0.33	7.15 ± 1.63 ^{ab}	Menopause <i>p</i> = 0.1039, diabetes <i>p</i> < 0.0001, interaction <i>p</i> = 0.8347
	MEG	108.28 ± 9.48	148.46 ± 31.48 _{ab}	121.24 ± 9.60	158.50 ± 45.88 ^{ab}	Menopause <i>p</i> = 0.1039, diabetes <i>p</i> < 0.0001, interaction <i>p</i> = 0.8347
	Trig	114.93 ± 33.00	190.71 ± 84.31	128.47 ± 54.56	142.08 ± 66.86	Menopause <i>p</i> = 0.2834, diabetes <i>p</i> = 0.0077, interaction <i>p</i> = 0.0600
	T Col	189.93 ± 47.30	175.86 ± 28.57	214.63 ± 38.56	184.17 ± 31.18	Menopause <i>p</i> = 0.1409, diabetes <i>p</i> = 0.0486, interaction <i>p</i> = 0.4617
	HDL	52.33 ± 9.10	52.57 ± 12.88	52.13 ± 8.55	49.42 ± 9.62	n/s
	LDL	121.6 ± 39.68	85.00 ± 29.25	139.77 ± 31.16	106.33 ± 26.06 ^b	Menopause <i>p</i> = 0.0366, diabetes <i>p</i> = 0.0004, interaction <i>p</i> = 0.8645
Hepatic parameters	OGT	24.73 ± 9.96	22.71 ± 7.27	24.27 ± 6.05	25.00 ± 5.31	Menopause <i>p</i> = 0.6582, diabetes <i>p</i> = 0.7544, interaction <i>p</i> = 0.5036
	GPT	20.93 ± 11.18	18.71 ± 6.75	19.97 ± 5.86	22.58 ± 15.00	Menopause <i>p</i> = 0.5974, diabetes <i>p</i> = 0.9423, interaction <i>p</i> = 0.3799
	GGT	24.4 ± 10.05	52.43 ± 27.63 ^{ab}	26.10 ± 10.04	32.17 ± 16.59 ^c	Menopause <i>p</i> = 0.0247, diabetes <i>p</i> < 0.0001, interaction <i>p</i> = 0.0084
	ALF	99.00 ± 27.15	87.43 ± 22.29	112.67 ± 34.11	109.25 ± 25.23	Menopausal <i>p</i> = 0.0428, diabetes <i>p</i> = 0.3856, interaction <i>p</i> = 0.6361
Oxidative and inflammatory parameters	MDA	0.02 ± 0.05	0.03 ± 0.04	0.007 ± 0.001	0.155 ± 0.0147 _{abc}	Menopause <i>p</i> = 0.0096, diabetes <i>p</i> = 0.0002, interaction <i>p</i> = 0.0008
	Leukometry	6.56 ± 1.57	6.21 ± 1.07	6.61 ± 1.58	8.50 ± 2.76 ^b	Menopause <i>p</i> = 0.0330, diabetes <i>p</i> = 0.1538, interaction <i>p</i> = 0.0412
	ESR	12.58 ± 10.30	38.86 ± 12.61	31.97 ± 26.13	29.17 ± 26.53	Menopause <i>p</i> = 0.4711, diabetes <i>p</i> = 0.0843, interaction <i>p</i> = 0.0337
	CRP	0.48 ± 0.59	0.77 ± 0.82	0.52 ± 0.47	0.61 ± 0.61	Menopause <i>p</i> = 0.7057, diabetes <i>p</i> = 0.2545, interaction <i>p</i> = 0.5432

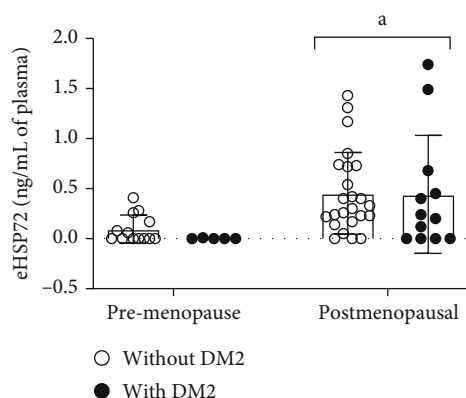


FIGURE 1: Plasma eHSP72 levels in premenopausal women without DM2 ($n = 13$) and with DM2 ($n = 05$) and postmenopausal women without DM2 ($n = 24$) and with DM2 ($n = 12$). Data were expressed in mean \pm standard deviation. Two-way ANOVA, followed by Tukey. Menopause $p = 0.0026$; diabetes $p = 0.6788$; interaction $p = 0.7374$. ^avs. premenopause.

affected by the interaction between menopause and DM2, although a multiple comparisons analysis did not indicate the difference between groups. Interestingly, the CRP levels were not responsive to menopause status or DM2 condition (Table 1).

Thus, we also analyzed eHSP72 levels as a biomarker of the inflammatory status. The chi-square test showed that 83.3% of the postmenopausal women presented detectable levels of circulating eHSP72, while only 50% of premenopausal women presented detectable levels ($p = 0.0048$). Besides, postmenopausal women (0.4494 ± 0.07804 , $n = 36$) presented higher eHSP72 levels compared to premenopausal women (0.07031 ± 0.02936 , $n = 18$), and this effect was independent of DM2 diagnosis (Figure 1). We stratified women according to their ages (group 27–59 years old and group 60–83 years old), considering the median age of the postmenopausal women. The eHSP72 levels did not differ among groups ($p = 0.0717$).

Following the comparison between our four initial groups, we implemented a detailed evaluation of the postmenopausal women's conditions. We performed a multivariate regression analysis of eHSP72 levels (dependent variable) and 17- β estradiol (E_2) levels, time of menopause, and DM2 diagnosis, considering only the postmenopausal women. We found that both factors affect the eHSP72 levels (Table 2).

The analysis of the association between eHSP72 and time of menopause reveals a curvilinear relationship between factors, with decreasing values over the first 11 years after menopause and subsequent elevation (Figure 2(a)). The line adjusts by the quadratic regression indicate a positive association between plasma eHSP72 and time of menopause ($R^2 0.23541$, $p = 0.0045$) (Figure 2(a)).

Further, we stratified postmenopausal women into two groups according to the median of the time of menopause. We established two groups: one composed of women with one to 11 years postmenopause, the other composed of women 12 to 29 years postmenopause. Thus, we analyzed

TABLE 2: Multivariate regression analysis between eHSP72, age, E_2 levels, time of menopause, and DM2 in postmenopausal women.

Variables	Multivariate regression ANOVA		
	R^2_{aj}	F	p
Age	0.48	7.945114	0.5143
E_2 levels			0.0018
Time of menopause			0.0152
DM2			0.0090

E_2 : 17- β estradiol (pg/mL); DM2: type II diabetes mellitus (absence = 0 and presence = 1); time of menopause and age (years). R^2_{aj} : R-adjusted square ($n = 31$).

in each group the correlation between eHSP72 and the time of menopause. We found a linear and positive association between eHSP72 levels and the time of menopause in women with 12 to 29 years of menopause ($R^2 0.33$; $p = 0.0248$; $r = 0.56$) (Figure 2(b)).

Thus, we confirmed these results by comparing the eHSP72 levels between the groups of postmenopausal (group 1–11 years of postmenopause and group 12–29 years of postmenopause) and the premenopausal women. Women 12 to 29 years of postmenopause presented higher eHSP72 levels than premenopausal women (Figure 3(a)). On the other hand, CRP did not differ between groups (Figure 3(b)). As expected, both postmenopausal groups presented lower E_2 levels compared to premenopausal women, but it was not affected by the time of menopause (Figure 3(c)).

4. Discussion

In our study, postmenopause was marked by increased eHSP72 levels, which were affected by the E_2 levels, DM2, and, most important, by the time of menopause. In addition, we found that menopause combined with DM2 predisposed to plasma oxidative damage and affected hepatic functions. Besides, postmenopause represented an additional risk factor for lipid homeostasis when not followed by pharmaceutical treatment. Therefore, our data support the hypothesis that eHSP72 can be a potential biomarker of the immune and inflammatory status in postmenopause conditions.

The complexity of the menopause period reflects in anthropometric, metabolic, and endocrine changes [20]. The gradual downfall of E_2 production by ovaries is usually followed by changes in body composition, such as the gradual decrease of muscle mass and the increase of adiposity, mainly centrally disposed [21]. Not surprisingly, 94% of the postmenopausal and 86% of premenopausal women from our study had abdominal circumference superior to 88 cm, which represents metabolic risk.

Obesity is an important risk factor for insulin resistance [22], although not necessary since hypoestrogenism per se influences glycemic homeostasis [23]. In our study, as expected, diabetic women presented higher fasting glycemia and HbA1c in pre- and postmenopause, without differing between menopausal status. Thus, we analyzed only healthy

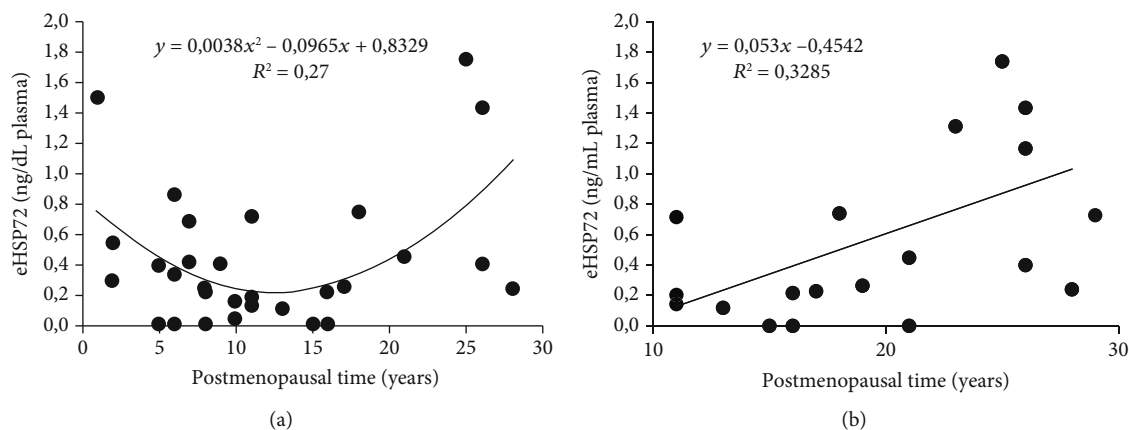


FIGURE 2: (a) Relation between eHSP72 levels and time of menopause. Positive correlation, linearized by quadratic regression ($n = 36$; $p = 0.0045$). (b) Relation between eHSP72 and the time of menopause in women 12 to 29 years postmenopause. Linear and simple regression, positive correlation ($n = 17$; $p = 0.0248$).

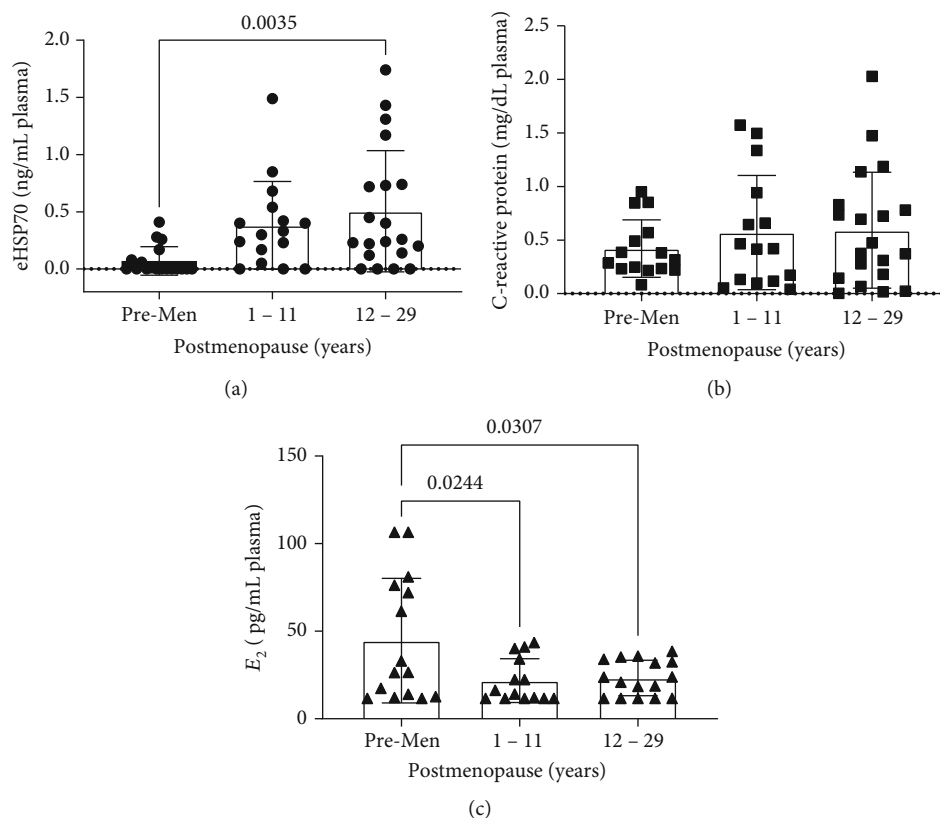


FIGURE 3: (a) eHSP7; (b) C-reactive protein (CRP); and (c) 17β -estradiol (E2) levels, in premenopausal (premen) ($n = 15 - 18$) and postmenopausal women 1 to 11 years ($n = 14 - 16$) and 12 to 29 years of postmenopause ($n = 17 - 20$). One-way ANOVA, followed by Tukey. ^avs. premenopausal woman, $p < 0.05$.

women (without DM2, normotensives, not currently using medications), and we found that HbA1 was higher in postmenopausal. In addition, 49% of “healthy” postmenopausal women were at risk (HbA1c between 5.7 and 6.4%) for DM2 development.

Besides the impairment in glycemic homeostasis, the occurrence of dyslipidemias secondary to the E2 downfall is common in postmenopausal women [24]. In our study, we did not find any effect of the postmenopause condition

on HDL levels. It may be related to the already reported dysfunctional HDL, followed by a compensatory increase in its levels in menopause conditions [25, 26]. Besides, LDL was also affected by menopause, but its levels were higher in women without DM2. These intriguing results may be related to the use of cholesterol-lowering medications, such as statins, which were associated with LDL levels. DM2 also affected triglycerides levels, as already described [27].

Diabetes increases the circulating levels of fatty acids, which can overload the liver. Thus, we evaluated the hepatic function by measuring hepatic enzymes. Although the GOT and GPT were unchanged, menopause enhanced ALF levels independent of DM2, and GGT was affected by both factors. Besides acting as a biomarker of hepatic function, GGT plays a role in intracellular glutathione synthesis and the antioxidant response [28]. Such antioxidant response may be impaired in DM2, which is marked by chronic and low-grade oxidative and inflammatory conditions that follow the metabolic alterations [29].

Accordingly, the postmenopausal women with DM2 presented the highest plasmatic lipoperoxidation levels. Estrogen, mainly 17β -estradiol (E2), is a powerful antioxidant [28] by modulating the expression and activity of several antioxidant enzymes. Thus, hypoestrogenism in postmenopause impairs the redox status [2, 30], which is exacerbated in diabetic women. We confirmed the association between lipoperoxidation and DM2 by performing a multivariate regression. Hence, these results show that menopause and DM2 present synergistic effects, and their association potentialize the risk of oxidative damage.

E2 is also a powerful anti-inflammatory hormone, and the lack of it represents a risk for the establishment of a chronic and low-grade inflammatory condition. In our study, menopause isolated and combined with DM2 enhanced the leukometry in a way that postmenopausal women with DM2 had the highest numbers. Leukocytosis mainly represents the enhancement of myeloid cell production and the number of circulating neutrophils and monocytes in senescence [31] and hyperglycemia, which mark the inflammatory status [31, 32]. Thus, the synergistic effects of menopause and DM2 found in our study support that postmenopausal women with DM2 are exposed to an additional risk for cardiovascular outcomes [33].

In agreement with that, the interaction between menopause and DM2 also affected ESR, a routinely used biomarker of inflammation. ESR does not respond quickly to the initial stages of the inflammatory process and remains elevated for longer periods than acute-phase proteins, such as CRP [34]. Interestingly, the CRP levels were not affected by these risk factors. CRP is an acute phase biomarker whose hepatic production and release are induced by IL-6 and TNF- α , highly available in menopause [35]. Besides, CRP is not just a biomarker but also a crucial factor in obesity development [36].

Despite being a well-recognized inflammatory biomarker, in our study, CRP was not affected by menopause nor diabetes. Since CRP was described as the strongest factor associated with overweight [37], the lack of responsiveness may be because the women participating in our study did not differ in anthropometric measurements despite the diabetes diagnosis. Thus, it led us to investigate whether HSP72 could be more sensitive to menopause plus diabetes low-grade inflammatory background.

HSP72 plays a fundamental role as a chaperone, anti-inflammatory, antioxidant, and antiapoptotic protein [38], whose expression is regulated by E2 [39, 40]. However, previous studies showed that a short and middle deprivation of

E2 does not downregulate HSP72 expression [41, 42], which suggests that the cellular response to stress during hypoestrogenism may depend on the time of postmenopause [43]. We found a curvilinear relationship between eHSP72 levels and the time of menopause, with decreasing values during the first 11 years and increasing values between 12 to 29 years of menopause. Thus, we stratified the postmenopausal women according to the time of menopause and found that the group with longer periods of postmenopause had high eHSP72 levels.

The time of postmenopause is naturally related to the lifespan. Considering that aging impairs the heat shock response, independent of E2 deprivation [43], we analyzed whether the eHSP72 levels in postmenopausal women could be related to their age rather than the time of menopause. Thus, we compared postmenopausal women younger (≤ 60 years) and older than 60 years old (≥ 60 years), and the eHSP72 levels did not differ among groups. These data reinforce the responsiveness of eHSP72 to the time of menopause, which may represent an attempt to restore the nitric oxide-HSP72 axis, highly required during estrogen downfall and in postmenopause [3].

In the extracellular medium, the importance of eHSP72 resides in warning signaling [9], immune-regulation, and mediating proinflammatory pathways [44, 45]. Moreover, eHSP72 levels correlate with the severity of atherosclerosis [46] and with the time of diagnosis of DM2 [47]. Until this moment, whether eHSP72 could help mark the complexity of the menopausal period was unclear. We showed that eHSP72 levels are also sensitive to the time of postmenopause and would be a potential biomarker of chronic conditions related to the metabolic impairment present in postmenopause. Besides, considering that the well-recognized inflammatory biomarker CRP [36, 37, 48] was not responsive in our study, we also suggest that in menopause plus diabetes low-grade inflammatory background, the serum eHSP72 levels may be more sensitive and a better biomarker of the preclinical stages.

5. Conclusion

The time of menopause enhances the plasmatic eHSP72 levels, which are also sensitive to E2 levels and DM2. Besides, menopause associated with DM2 is marked by an additional risk of systemic oxidative damage. Together, menopause and DM2 present synergistic effects in metabolic, oxidative, and inflammatory parameters and require special attention. Most important, in menopause plus DM2 chronic low-grade inflammatory background, eHSP72 levels can be a potential biomarker and a better alternative of follow-up than well-established biomarkers.

Data Availability

The datasets used and/or analyzed during the current study are available from the corresponding author upon reasonable request.

Conflicts of Interest

The authors declare no conflicts of interest.

Authors' Contributions

CFVA, YPSL, and MNF completed all the interviews, blood collection, and biochemical analysis. CFVA, LMS, MSL, and TGH performed the statistical analysis. ABS, LCCB, and LMS performed lipoperoxidation and HSP72 analysis. LCCB, MNF, PBGF, TGH, and MSL cowrote the manuscript. All the authors approved the final version.

Acknowledgments

This study was supported by the Regional University of Northwestern Rio Grande do Sul State (UNIJUÍ).

References

- [1] D. A. Schoenaker, C. A. Jackson, J. V. Rowlands, and G. D. Mishra, "Socioeconomic position, lifestyle factors and age at natural menopause: a systematic review and meta-analyses of studies across six continents," *International Journal of Epidemiology*, vol. 43, no. 5, pp. 1542–1562, 2014.
- [2] M. A. Sanchez-Rodriguez, M. Zacarias-Flores, A. Arronte-Rosales, E. Correa-Munoz, and V. M. Mendoza-Nunez, "Menopause as risk factor for oxidative stress," *Menopause*, vol. 19, no. 3, pp. 361–367, 2012.
- [3] A. A. Miragem and P. I. Homem de Bittencourt Jr., "Nitric oxide-heat shock protein axis in menopausal hot flushes: neglected metabolic issues of chronic inflammatory diseases associated with deranged heat shock response," *Human Reproduction Update*, vol. 23, no. 5, pp. 600–628, 2017.
- [4] Y. Liu, J. Ding, T. L. Bush et al., "Relative androgen excess and increased cardiovascular risk after menopause: a hypothesized relation," *American Journal of Epidemiology*, vol. 154, no. 6, pp. 489–494, 2001.
- [5] P. Newsholme, V. F. Cruzat, K. N. Keane, R. Carlessi, and P. I. H. de Bittencourt Jr., "Molecular mechanisms of ROS production and oxidative stress in diabetes," *The Biochemical Journal*, vol. 473, no. 24, pp. 4527–4550, 2016.
- [6] D. Jedrzejuk and A. Milewicz, "Consequences of menopause in women with diabetes mellitus - a clinical problem," *Gynecological endocrinology: the official journal of the International Society of Gynecological Endocrinology*, vol. 21, no. 5, pp. 280–286, 2005.
- [7] A. P. Arruda, M. Milanski, A. Coepe et al., "Low-grade hypothalamic inflammation leads to defective thermogenesis, insulin resistance, and impaired insulin secretion," *Endocrinology*, vol. 152, no. 4, pp. 1314–1326, 2011.
- [8] T. G. Heck, S. P. Scomazzon, P. R. Nunes et al., "Acute exercise boosts cell proliferation and the heat shock response in lymphocytes: correlation with cytokine production and extracellular-to-intracellular HSP70 ratio," *Cell Stress & Chaperones*, vol. 22, no. 2, pp. 271–291, 2017.
- [9] H. E. Ireland, F. Leoni, O. Altaie et al., "Measuring the secretion of heat shock proteins from cells," *Methods*, vol. 43, no. 3, pp. 176–183, 2007.
- [10] C. Boudesco, S. Cause, G. Jago, and C. Garrido, "Hsp 70: a cancer target inside and outside the cell," *Methods in Molecular Biology*, vol. 1709, pp. 371–396, 2018.
- [11] M. M. Sulzbacher, M. S. Ludwig, and T. G. Heck, "Oxidative stress and decreased tissue HSP70 are involved in the genesis of sepsis: HSP70 as a therapeutic target," *Revista Brasileira de terapia intensiva*, vol. 32, no. 4, pp. 585–591, 2020.
- [12] E. A. Nahas, J. Nahas-Neto, C. L. Orsatti, M. L. Sobreira, A. P. Tardivo, and S. S. Witkin, "Evaluation of clinical and inflammatory markers of subclinical carotid atherosclerosis in postmenopausal women," *Menopause*, vol. 21, no. 9, pp. 982–989, 2014.
- [13] A. G. Pockley, B. Henderson, and G. Multhoff, "Extracellular cell stress proteins as biomarkers of human disease," *Biochemical Society Transactions*, vol. 42, no. 6, pp. 1744–1751, 2014.
- [14] M. Nakhjavani, A. Morteza, A. Meysamie et al., "Serum heat shock protein 70 and oxidized LDL in patients with type 2 diabetes: does sex matter?," *Cell Stress & Chaperones*, vol. 16, no. 2, pp. 195–201, 2011.
- [15] Diabetes SBD, "Conduta Terapêutica no Diabetes Tipo 2: Algoritmo SBD 2015," May 2021, <http://www.diabetes.org.br/profissionais/images/2017/posicionamento-2.pdf>.
- [16] ABESO, "Diretrizes Brasileiras de Obesidade," 2016, <http://abeso.org.br/wp-content/uploads/2019/12/Diretrizes-Download-Diretrizes-Brasileiras-de-Obesidade-2016.pdf>.
- [17] R. N. Bergman, D. Stefanovski, T. A. Buchanan et al., "A better index of body adiposity," *Obesity*, vol. 19, no. 5, pp. 1083–1089, 2011.
- [18] A. C. Sposito, B. Caramelli, F. A. Fonseca et al., "IV Diretriz Brasileira sobre Dislipidemias e Prevenção da Aterosclerose," *Arquivos Brasileiros de Cardiologia*, vol. 88, pp. 2–19, 1997.
- [19] J. A. Buege and S. D. Aust, "[30] Microsomal lipid peroxidation," *Methods in Enzymology*, vol. 52, pp. 302–310, 1978.
- [20] J. Medina-Contreras, R. Villalobos-Molina, A. Zarain-Herzberg, and J. Balderas-Villalobos, "Ovariectomized rodents as a menopausal metabolic syndrome model. A minireview," *Molecular and Cellular Biochemistry*, vol. 475, no. 1–2, pp. 261–276, 2020.
- [21] D. S. Bendale, P. A. Karpe, R. Chhabra, S. P. Shete, H. Shah, and K. Tikoo, "17-β Oestradiol prevents cardiovascular dysfunction in post-menopausal metabolic syndrome by affecting SIRT1/AMPK/H3 acetylation," *British Journal of Pharmacology*, vol. 170, no. 4, pp. 779–795, 2013.
- [22] P. Newsholme and P. I. H. de Bittencourt Jr., "The fat cell senescence hypothesis: a mechanism responsible for abrogating the resolution of inflammation in chronic disease," *Current Opinion in Clinical Nutrition and Metabolic Care*, vol. 17, no. 4, pp. 295–305, 2014.
- [23] Y. Heianza, Y. Arase, S. Kodama et al., "Effect of postmenopausal status and age at menopause on type 2 diabetes and pre-diabetes in Japanese individuals: Toranomon Hospital Health Management Center Study 17 (TOPICS 17)," *Diabetes Care*, vol. 36, no. 12, pp. 4007–4014, 2013.
- [24] J. C. Stevenson, S. Tsiligiannis, and N. Panay, "Cardiovascular risk in perimenopausal women," *Current Vascular Pharmacology*, vol. 17, no. 6, pp. 591–594, 2019.
- [25] S. R. El Khoudary, "HDL and the menopause," *Current Opinion in Lipidology*, vol. 28, no. 4, pp. 328–336, 2017.
- [26] S. R. El Khoudary, P. M. Hutchins, K. A. Matthews et al., "Cholesterol efflux capacity and subclasses of HDL particles in healthy women transitioning through menopause," *The*

- Journal of Clinical Endocrinology and Metabolism*, vol. 101, no. 9, pp. 3419–3428, 2016.
- [27] B. Bhowmik, T. Siddiquee, A. Mujumder et al., “Serum lipid profile and its association with diabetes and prediabetes in a rural Bangladeshi population,” *International Journal of Environmental Research and Public Health*, vol. 15, no. 9, p. 1944, 2018.
- [28] C. C. C. Mendoza and C. A. J. Zamarripa, “Menopause induces oxidative stress,” in *Oxidative Stress and Chronic Degenerative Diseases - A Role for Antioxidants*, J. A. Morales-González, Ed., InTech, 2013.
- [29] A. Picu, L. Petcu, S. Stefan et al., “Markers of oxidative stress and antioxidant defense in Romanian patients with type 2 diabetes mellitus and obesity,” *Molecules*, vol. 22, no. 5, p. 714, 2017.
- [30] B. L. Crist, D. L. Alekel, L. M. Ritland, L. N. Hanson, U. Genschel, and M. B. Reddy, “Association of oxidative stress, iron, and centralized fat mass in healthy postmenopausal women,” *Journal of Women's Health*, vol. 18, no. 6, pp. 795–801, 2009.
- [31] M. Nahrendorf, “Myeloid cell contributions to cardiovascular health and disease,” *Nature Medicine*, vol. 24, no. 6, pp. 711–720, 2018.
- [32] P. R. Nagareddy, A. J. Murphy, R. A. Stirzaker et al., “Hyperglycemia promotes myelopoiesis and impairs the resolution of atherosclerosis,” *Cell Metabolism*, vol. 17, no. 5, pp. 695–708, 2013.
- [33] M. Madjid, I. Awan, J. T. Willerson, and S. W. Casscells, “Leukocyte count and coronary heart disease: implications for risk assessment,” *Journal of the American College of Cardiology*, vol. 44, no. 10, pp. 1945–1956, 2004.
- [34] C. Bray, L. N. Bell, H. Liang et al., “Erythrocyte sedimentation rate and C-reactive protein measurements and their relevance in clinical medicine,” *WMJ: official publication of the State Medical Society of Wisconsin*, vol. 115, no. 6, pp. 317–321, 2016.
- [35] S. M. Conroy, H. K. Neilson, R. O'Reilly et al., “Associations between postmenopausal endogenous sex hormones and C-reactive protein: a clearer picture with regional adiposity adjustment?,” *Menopause*, vol. 24, no. 9, pp. 1040–1048, 2017.
- [36] Q. Li, Q. Wang, W. Xu et al., “C-reactive protein causes adult-onset obesity through chronic inflammatory mechanism,” *Frontiers in Cell and Developmental Biology*, vol. 8, p. 18, 2020.
- [37] N. J. Timpson, B. G. Nordestgaard, R. M. Harbord et al., “C-reactive protein levels and body mass index: elucidating direction of causation through reciprocal Mendelian randomization,” *International Journal of Obesity*, vol. 35, no. 2, pp. 300–308, 2011.
- [38] L. C. Costa-Beber, G. E. Hirsch, T. G. Heck, and M. S. Ludwig, “Chaperone duality: the role of extracellular and intracellular HSP70 as a biomarker of endothelial dysfunction in the development of atherosclerosis,” *Archives of Physiology and Biochemistry*, vol. 15, pp. 1–8, 2020.
- [39] D. Manthey and C. Behl, “From structural biochemistry to expression profiling: neuroprotective activities of estrogen,” *Neuroscience*, vol. 138, no. 3, pp. 845–850, 2006.
- [40] A. A. Knowlton and L. Sun, “Heat-shock factor-1, steroid hormones, and regulation of heat-shock protein expression in the heart,” *American Journal of Physiology. Heart and Circulatory Physiology*, vol. 280, no. 1, pp. H455–H464, 2001.
- [41] Y. P. S. Lissarassa, C. F. Vincensi, L. C. Costa-Beber et al., “Chronic heat treatment positively impacts metabolic profile of ovariectomized rats: association with heat shock response pathways,” *Cell Stress & Chaperones*, vol. 25, no. 3, pp. 467–479, 2020.
- [42] A. A. Miragem, M. S. Ludwig, T. G. Heck et al., “Estrogen deprivation does not affect vascular heat shock response in female rats: a comparison with oxidative stress markers,” *Molecular and Cellular Biochemistry*, vol. 407, no. 1–2, pp. 239–249, 2015.
- [43] Y. Hou, H. Wei, Y. Luo, and G. Liu, “Modulating expression of brain heat shock proteins by estrogen in ovariectomized mice model of aging,” *Experimental Gerontology*, vol. 45, no. 5, pp. 323–330, 2010.
- [44] L. C. Costa Beber, M. da Silva, A. B. dos Santos et al., “The association of subchronic exposure to low concentration of PM2.5 and high-fat diet potentiates glucose intolerance development, by impairing adipose tissue antioxidant defense and eHSP72 levels,” *Environmental Science and Pollution Research International*, vol. 27, no. 25, pp. 32006–32016, 2020.
- [45] C. H. de Lemos Muller, A. Rech, C. E. Botton et al., “Heat-induced extracellular HSP72 release is blunted in elderly diabetic people compared with healthy middle-aged and older adults, but it is partially restored by resistance training,” *Experimental Gerontology*, vol. 111, pp. 180–187, 2018.
- [46] F. Xie, R. Zhan, L. C. Yan et al., “Diet-induced elevation of circulating HSP70 may trigger cell adhesion and promote the development of atherosclerosis in rats,” *Cell Stress & Chaperones*, vol. 21, no. 5, pp. 907–914, 2016.
- [47] M. Nakhjavani, A. Morteza, L. Khajeali et al., “Increased serum HSP70 levels are associated with the duration of diabetes,” *Cell Stress & Chaperones*, vol. 15, no. 6, pp. 959–964, 2010.
- [48] M. B. Pepys, G. M. Hirschfield, G. A. Tennent et al., “Targeting C-reactive protein for the treatment of cardiovascular disease,” *Nature*, vol. 440, no. 7088, pp. 1217–1221, 2006.

Research Article

ROS-ERK Pathway as Dual Mediators of Cellular Injury and Autophagy-Associated Adaptive Response in Urinary Protein-Irritated Renal Tubular Epithelial Cells

Jian-kun Deng,¹ Xueqin Zhang ,² Hong-luan Wu,¹ Yu Gan,¹ Ling Ye,¹ Huijuan Zheng,² Zebing Zhu,² Wei Jing Liu ,^{1,2} and Hua-feng Liu ¹

¹Institute of Nephrology, Zhanjiang Key Laboratory of Prevention and Management of Chronic Kidney Disease, Guangdong Medical University, Zhanjiang, Guangdong 524001, China

²Renal Research Institution of Beijing University of Chinese Medicine, and Key Laboratory of Chinese Internal Medicine of Ministry of Education and Beijing, Dongzhimen Hospital Affiliated to Beijing University of Chinese Medicine, Beijing 100700, China

Correspondence should be addressed to Wei Jing Liu; liuweijing-1977@hotmail.com and Hua-feng Liu; hf-liu@263.net

Received 29 October 2020; Revised 11 January 2021; Accepted 8 February 2021; Published 2 March 2021

Academic Editor: Shikha Tewari

Copyright © 2021 Jian-kun Deng et al. This is an open access article distributed under the Creative Commons Attribution License, which permits unrestricted use, distribution, and reproduction in any medium, provided the original work is properly cited.

ERK, an extracellular signal-regulated protein kinase, is involved in various biological responses, such as cell proliferation and differentiation, cell morphology maintenance, cytoskeletal construction, apoptosis, and canceration of cells. In this study, we focused on ERK pathway on cellular injury and autophagy-associated adaptive response in urinary protein-irritated renal tubular epithelial cells and explored the potential mechanisms underlying it. By using antioxidants N-acetylcysteine and catalase, we found that ERK pathway was activated by a reactive oxygen species- (ROS-) dependent mechanism after exposure to urinary proteins. What is more, ERK inhibitor U0126 could decrease the release of neutrophil gelatinase-associated lipocalin (NGAL), kidney injury molecule-1 (KIM-1), and the number of apoptotic cells induced by urinary proteins, indicating the damaging effects of ERK pathway in mediating cellular injury and apoptosis in HK-2 cells. Interestingly, we also found that the increased expression of microtubule-associated protein 1 light chain 3 (LC3)-II (a key marker of autophagy) and the decreased expression of p62 (autophagic substrate) induced by urinary proteins were reversed by U0126, suggesting autophagy was activated by ERK pathway. Furthermore, rapamycin reduced urinary protein-induced NGAL and KIM-1 secretion and cell growth inhibition, while chloroquine played the opposite effect, indicating that autophagy activation by ERK pathway was an adaptive response in the exposure to urinary proteins. Taken together, our results indicate that activated ROS-ERK pathway can induce cellular injury and in the meantime provide an autophagy-associated adaptive response in urinary protein-irritated renal tubular epithelial cells.

1. Introduction

Renal tubular epithelial cell injury is central to the pathophysiology of tubulointerstitial fibrosis, which strongly correlates with the decline of renal function [1–3]. Urinary protein, as a pathological product of glomerular diseases, is also an important factor leading to renal tubular epithelial cell injury. It is proved to cause cellular apoptosis, resulting in the detachment of renal tubular epithelial cells from the basement membrane and finally losing their functions to the renal tubules [4, 5]. Unfortunately, the underlying mech-

anisms of renal tubular epithelial injury induced by urinary protein remains unclear, limiting the research on effective therapy. Thus, it is of great importance to further explore the mechanism of urinary protein-induced cellular injury.

One of the important ways that urinary protein causes cellular injury is by elevating the production of reactive oxygen species (ROS) [6]. Moreover, ROS regulates various cellular signaling pathways, such as the ERK pathway [7]. With the phosphorylation of the Ras/Raf/MEK/ERK cascade, the ERK pathway is activated and participates in the regulation of a variety of cellular processes, which includes

proliferation, transdifferentiation, autophagy, and apoptosis [8–10]. However, the role of ERK pathway in renal injury is still controversial until now. The ERK pathway has proved to be a pathogenic factor in various disease models, such as cystic kidney diseases [11], kidney stones [12], and unilateral ureter obstruction kidneys [13, 14]. More directly, Reich et al. indicated that the ERK pathway mediates the albumin-induced toxicity of TECs [15]. In contrast, Takase et al. demonstrated that the ERK pathway could serve as an important prosurvival factor to TECs under protein overload [16]. And recent studies verified that ERK pathway-mediated autophagy was protective in podocyte damage caused by lipopolysaccharide [17]. Given the wide range functions of ERK pathway, we hypothesized that it may play different roles simultaneously under the same condition. Hence, the aim of the study is to determine the exact role of ERK pathway in renal tubular epithelial cells irritated by urinary protein and provide a theoretical basis for the treatment of renal injury caused by urinary proteins.

2. Materials and Methods

2.1. Extraction of Urinary Proteins. Ammonium sulfate precipitation method as described previously [18] was used to extract the urinary proteins from untreated patients pathologically diagnosed as minimal change nephrotic syndrome (MCNS).

2.2. Cell Culture and Treatments. Human proximal tubular HK-2 cells (ATCC, Manassas, VA) were maintained in Dulbecco's modified Eagle's medium (DMEM, Gibco, Grand Island, NY) supplemented with 10% fetal bovine serum (Gibco) under standard conditions. The cells were pretreated with 10 mM N-acetylcysteine (NAC) (Beyotime Institute of Biotechnology, Jiangsu), 2000 U/ml catalase (Beyotime Institute of Biotechnology, Jiangsu), 10 μ M U0126 (Sigma, St. Louis, MO), 10 μ M rapamycin (Calbiochem, La Jolla, CA, USA), and 10 μ M chloroquine (Sigma) before the addition of urinary proteins (8 g/l). The cellular ROS production was measured at 2 h, and the expression of LC3 and P62 was quantified at 8 h. The levels of neutrophil gelatinase-associated lipocalin (NGAL) and kidney injury molecule-1 (KIM-1) secretion were tested at 12 h with the Quantikine™ kits (R&D Systems, Minneapolis, Minnesota, USA). The number of apoptotic cells was assayed at 48 h. And the expression of p-ERK and t-ERK was quantified at different time points.

2.3. Flow Cytometry Analysis. Cell apoptosis determination and cellular ROS production were measured with flow cytometry. All cells under various experimental conditions were harvested at 48 h with culture solution containing 0.05 trypsin and rinsed with PBS. Apoptosis was determined by the AnnexinV-FITC Apoptosis Detection Kit (Dojindo, Kumamoto, Japan) following the manufacturer's protocol with FACS Calibur flow cytometer (BD, FACSCanto II, San Jose, CA). For ROS measurement, HK-2 cells were incubated with DMEM containing 10 μ M 2',7'-Dichlorodihydrofluorescein diacetate (DCFH-DA, Beyotime Institute of Bio-

technology, Jiangsu) for 30 min in the dark. Then, harvested cells were trypsinized and resuspended in PBS. The fluorescence was determined by FACS Calibur flow cytometer (BD, FACSCanto II, San Jose, CA).

2.4. Western Blot. Autophagy response and ERK pathway were both examined by Western blot. At the end of incubation, cells were washed with PBS and lysed on ice for 15 min in 1 \times RIPA lysis buffer. Conditioned media and cell lysates were centrifuged at 13,000 rpm at 4°C for 15 min to pellet cell debris, and the concentration of cellular protein was determined using BCA reagent. Samples with equal concentrations of cellular protein were mixed with a 5 \times sample buffer and heated at 95°C for 10 min and separated on 12% SDS-PAGE gels. The samples were then transferred to a polyvinylidene difluoride membrane (Millipore, Billerica, MA, USA). After blocking with 5% fat-free milk for 2 h, the membranes were incubated overnight at 4°C with rabbit antibodies raised against microtubule-associated protein 1 light chain 3 (LC3)-II (Sigma, St. Louis, MO), p62/SQSTM1 (Santa Cruz Biotechnology, Santa Cruz, CA), p-ERK (Cell Signaling Technology, Danvers, MA), and t-ERK (Cell Signaling Technology, Danvers, MA). After washing, the membranes were probed with HRP-conjugated secondary antibodies (Beyotime Institute of Biotechnology, Jiangsu) for 1 hour at room temperature. Immunoreactive bands were visualized using ECL plus Western blotting detection system (Pierce, Rockford, IL).

2.5. Cell Viability Assay. Cells were incubated with 5 mg/ml methyl thiazolyl tetrazolium (MTT) solution (Calbiochem) for 4 h at 37°C. The formazan crystals were dissolved in dimethylsulfoxide. Optical density was determined at 570 nm with a plate reader (Thermo Labsystems, Multiskan MK3, Shanghai, China).

2.6. Statistical Analysis. All statistical tests were performed with SPSS 16.0. Shapiro-Wilk test was used to detect the normality of variables. All data are expressed as the means \pm standard error of the mean (S.E.M.). Multiple group comparison was carried out using ANOVA, followed by Bonferroni post hoc tests. *P* value was considered as statistically significant if it was less than 0.05.

3. Results

3.1. ERK Pathway in TECs Was Activated by Oxidative Stress after Exposure to Urinary Proteins. In this study, we first evaluated the activity of ERK pathway by examining the expression of phosphorylated ERK (p-ERK), a key marker of ERK pathway activation. As shown in Figure 1, the expression of p-ERK was significantly increased in TECs after treatment with urinary protein at 2 h, suggesting the activation of ERK pathway after urinary protein overload. Meanwhile, we found that the ROS production was remarkably elevated. Subsequently, to clarify the relationship between ERK pathway activation and ROS overproduction, we pretreated protein overload HK-2 cells with antioxidants (NAC and CAT). The results of flow cytometry and Western blot showed that the expression of p-ERK decreased with the

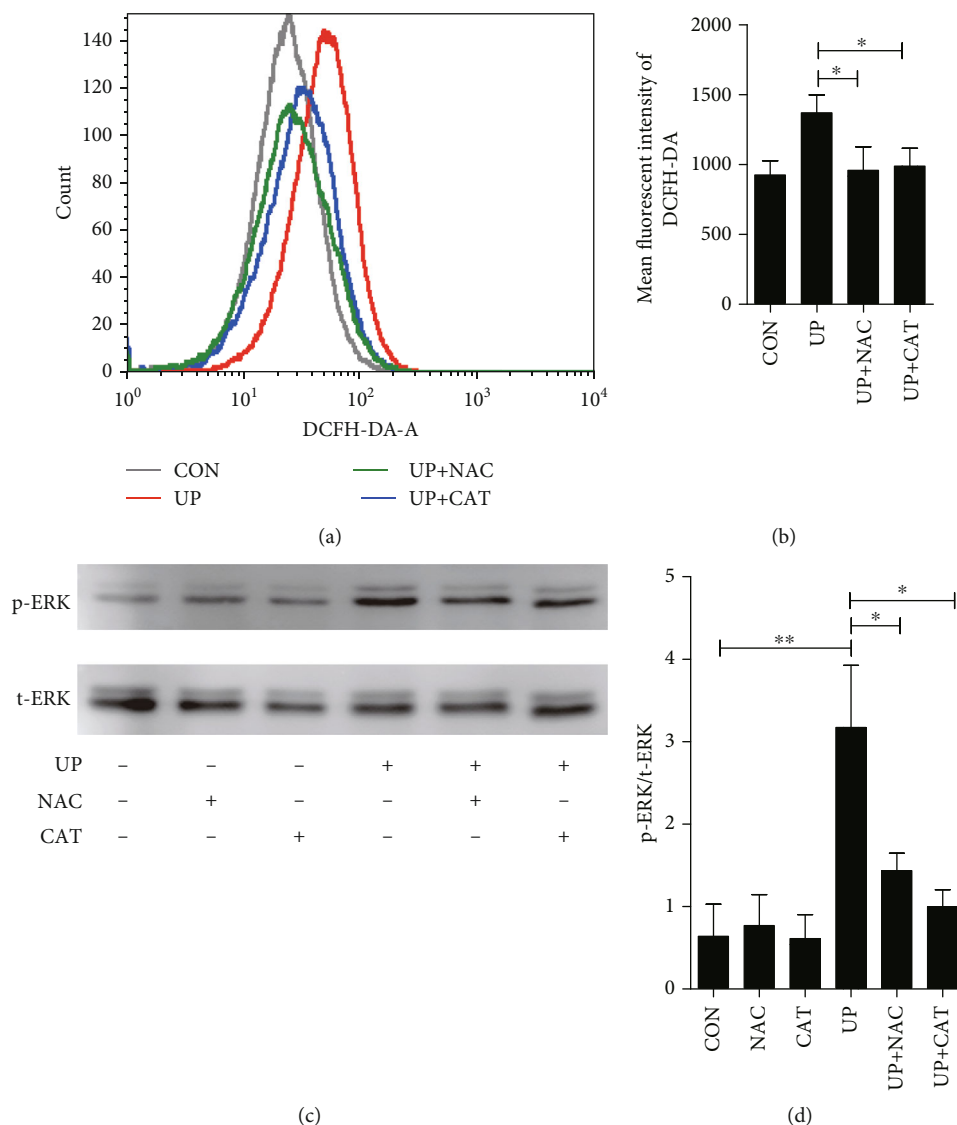


FIGURE 1: Effect of antioxidants on urinary protein-induced ERK pathway activation. Antioxidants NAC (10 mM) and CAT (2000 U/ml) were administered 1 h before the addition of 8 mg/ml urinary proteins for 2 h. Cell culture supernatant was subjected to DCFH-DA flow cytometry analysis of ROS levels (a, b). After treatment with urinary proteins for 4 h, aliquots of cell lysate were subjected to Western blot analysis of p-ERK and t-ERK level (c, d). (b) $F(3,8) = 4.901$; (d) $F(5,12) = 5.581$. * $P < 0.05$ and ** $P < 0.01$. CON: control; NAC: N-acetylcysteine; CAT: catalase; UP: urinary proteins.

application of antioxidants. Collectively, these results demonstrated that ERK pathway was activated in urinary-treated TECs and mediated by a ROS-dependent mechanism.

3.2. ERK Pathway Activation Was Involved in Urinary Protein-Induced TEC Injury. Since previous studies have shown that exposure to urinary proteins resulted in injury and even apoptosis in HK-2 cells, we then intended to further explore whether the ERK pathway was the responsible process. Firstly, the inhibiting effect of an ERK inhibitor U0126 on ERK pathway was tested by Western blot. As shown in Figures 2(a) and 2(b), pretreatment with U0126 could effectively suppress the expression of p-ERK, suggesting effective blockage of U0126 in activated ERK pathway. Then, we evaluated the early and late apoptosis by coupled staining with

FITC annexin V and PI. The results showed that ERK inhibitor could attenuate cellular apoptosis induced by urinary proteins (Figures 2(c) and 2(d)). Furthermore, U0126 reduced the level of tubular injury markers NGAL and KIM-1, which have been increased with urinary protein stimulation (Figures 2(e) and 2(f)). These results indicated that ERK pathway activation caused by urinary protein led to cellular injury and apoptosis in HK-2 cells.

3.3. Autophagic Response Was Triggered by ERK Pathway after Exposure of TECs to Urinary Proteins. As our previous research has found that the cellular autophagy was activated by exposure to urinary proteins, the exact role of ERK pathway played in autophagy activation was further explored in this study. As shown in Figure 3, the amount of p62 had no

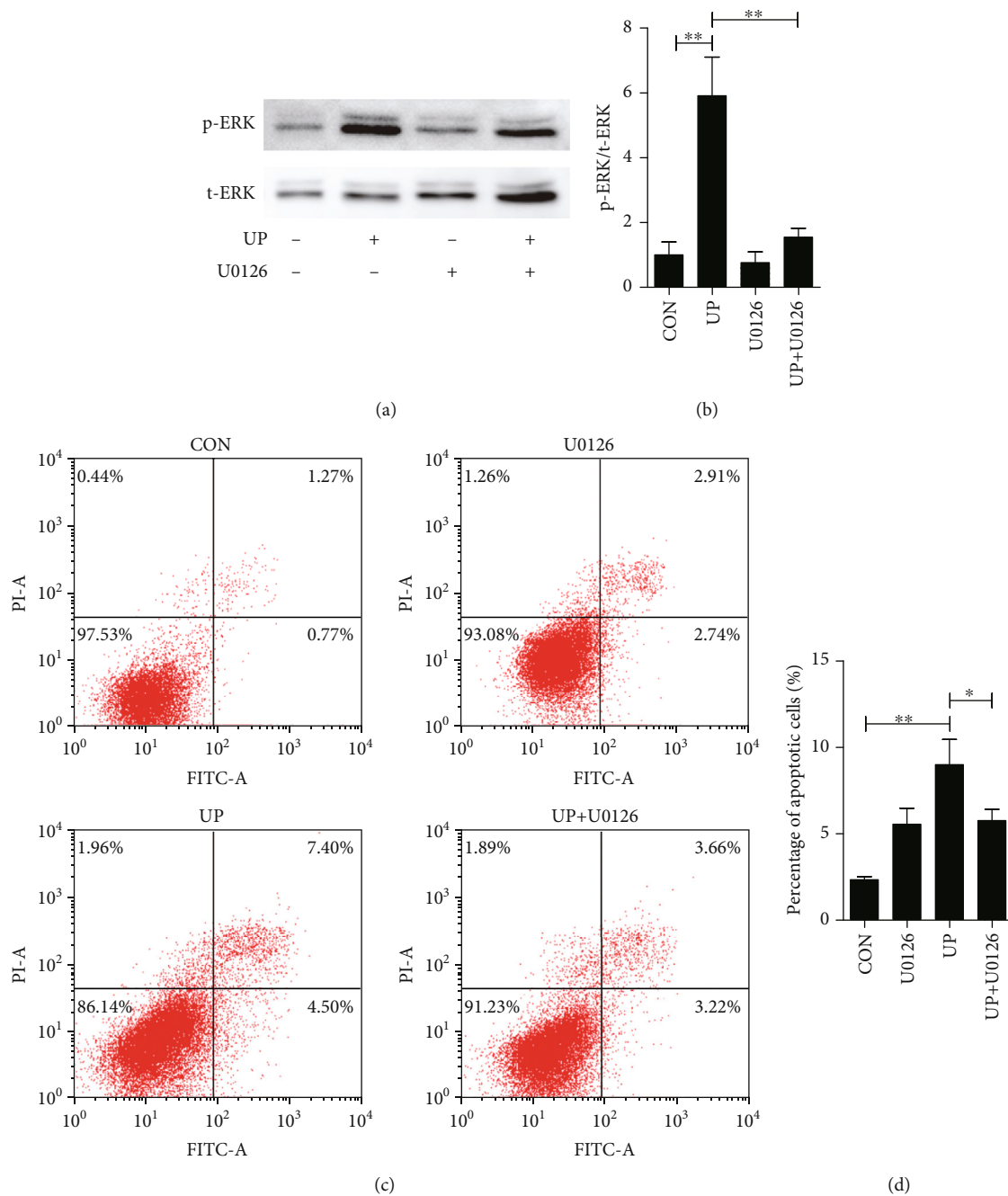


FIGURE 2: Continued.

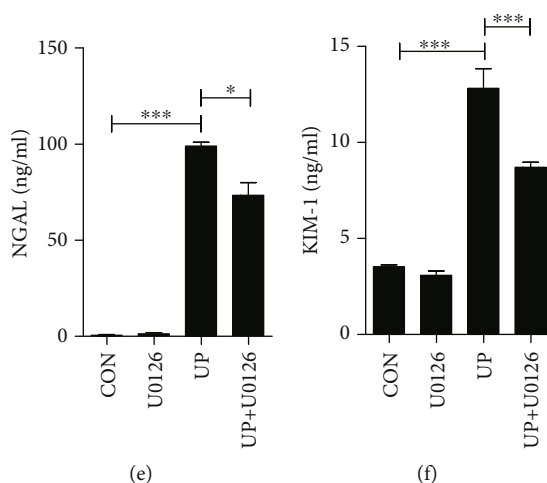


FIGURE 2: Effect of MEK inhibitor on urinary protein-induced injury. MEK inhibitor U0126 ($10 \mu\text{M}$) was administered 1 h before the addition of 8 g/l urinary proteins. The aliquots of cell lysate were subjected to Western blot analysis of p-ERK and t-ERK levels (a, b), and cellular apoptosis was assessed by Annexin V-FITC/PI flow cytometry analysis (c, d) at 48 h. Cell culture supernatant was subjected to ELISA analysis of the NGAL and KIM-1 secretion at 12 h (e, f). (b) $F(3, 8) = 13.385$; (d) $F(3, 8) = 8.539$; (e) $F(3, 12) = 207.111$; (f) $F(3, 16) = 72.157$. * $P < 0.05$, ** $P < 0.01$, and *** $P < 0.001$. CON: control; UP: urinary proteins.

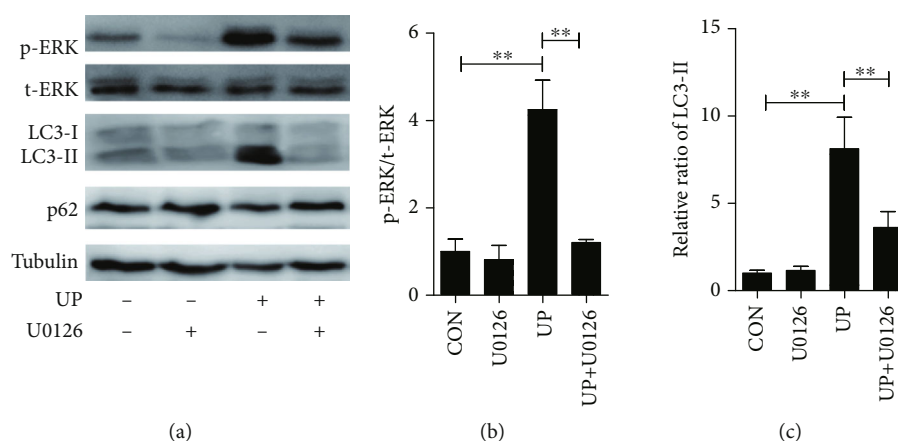


FIGURE 3: Effect of MEK inhibitor on urinary protein-induced autophagy. MEK inhibitor U0126 ($10 \mu\text{M}$) was administered 1 h before the addition of 8 g/l urinary proteins for 8 h. Aliquots of cell lysate were subjected to Western blot analysis of p-ERK, t-ERK, LC3, and p62 levels. (b) $F(3, 12) = 16.329$; (c) $F(3, 8) = 11.229$. ** $P < 0.01$. CON: control; UP: urinary proteins.

significant change but the amount of LC3-II was remarkably increased after exposure to urinary protein for 8 h, indicating the activation of autophagy. However, these effects could be eliminated by suppressing the expression of p-ERK with U0126, suggesting that autophagy activation by urinary protein was definitely ERK pathway dependent.

3.4. Adaptive Autophagic Response Alleviated TEC Injury Induced by Urinary Proteins. We next evaluated the role of autophagy in TEC injury. It is well known that rapamycin increases autophagy flux, while chloroquine blocks autophagy pathway. Thus, whether rapamycin or chloroquine affected the urinary protein-induced cellular injury was examined. We found that increased NGAL and KIM-1 release (Figures 4(a) and 4(b)) and growth inhibition (Figure 4(c)) were reduced by rapamycin, while opposite results were obtained with chloroquine when assessing

KIM-1 secretion. These findings indicated that autophagic response activated by ERK pathway was adaptive, for it could attenuate renal tubular injury caused by urinary proteins.

4. Discussion

In the present study, we demonstrated that ERK pathway was activated by a ROS-dependent mechanism in TEC cells exposed to urinary protein. What is more, it was proved to play dual roles in the cellular injury. On the one hand, it caused cellular injury directly; on the other hand, it could induce adaptive autophagic response to relieve the cellular injury. The complexity of the ROS-ERK pathway in TEC cells under condition of urinary protein overload was clarified for the first time.

ERK pathway is involved in various cellular processes [19]. In the present study, the results showed that once

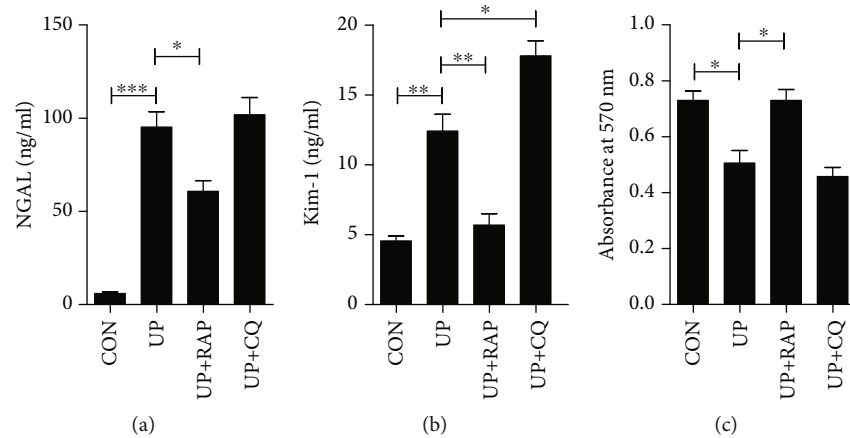


FIGURE 4: Effects of rapamycin or chloroquine on damage to TECs induced by urinary protein. (a, b) The levels of supernatant NGAL and KIM-1 were measured by ELISA after exposure to vehicle, urinary proteins (UP, 8 mg/ml), UP (8 mg/ml) plus rapamycin (RAP, 10 μ M), or UP (8 mg/ml) plus chloroquine (CQ, 10 μ M). (c) Cell proliferation was assessed by MTT assay as described in (a). * P < 0.05, ** P < 0.01. CON: control; UP: urinary proteins; RAP: rapamycin; CQ: chloroquine.

ERK activity was inhibited, urinary protein-induced TEC apoptosis and the release of factors that causes renal injury were reduced, suggesting the unfavorable role of ERK pathway in the process. However, the mechanism by which ERK pathway specifically mediates cell injury is currently unclear; it may be related to mitochondrial dysfunction [20, 21] or suppression of the Akt pathway which is positive to cell survival [22]. Notably, ERK inhibitor U0126 failed to completely block urinary protein-induced cell damage, suggesting that a non-ERK pathway may also be involved in mediating the toxicity of urinary proteins.

Previous studies have shown that urinary proteins could induce endoplasmic reticulum stress and mitochondrial dysfunction in TECs, resulting in massive ROS production [23, 24]. As an important intracellular messenger, ROS activates the ERK pathway via stimulation of EGF and PDGF receptors [25, 26] or by the way of oxidizing C118 residues in Ras directly [27]. Meanwhile, ROS could inhibit ERK-specific phosphatase activity and reduce the degradation of phosphorylated ERK [25]. Consistent with these studies, our study found that while urinary proteins stimulated large amounts of ROS generation, the ERK pathway of TECs was activated in TECs. Besides, inhibition dose of ROS in vitro, NAC, and CAT could block the activation of ERK. These results led us to conclude that oxidative stress induced by urinary protein is extremely significant for ERK pathway activation.

The ERK pathway has long been considered to be an important regulatory pathway for cellular autophagy [28]. Wang and Zeng have illustrated that ERK pathway could induce autophagy through Beclin 1 [29, 30]. Therefore, we posited that ERK pathway was involved in autophagy behavior and confirmed this hypothesis through protein overload model of cultured TECs. Using experimental methods consistent with our previous studies, we found that the expression of LC3-II was significantly increased, and the expression of autophagic substrate p62 was decreased after ERK pathway activation. As p62 is selectively incorporated into autophagosomes and is efficiently degraded by autophagy,

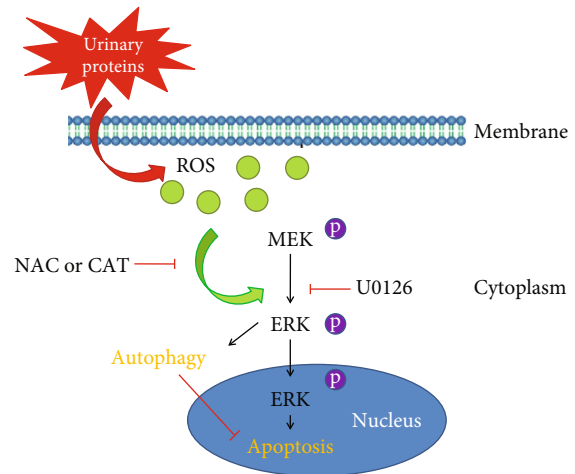


FIGURE 5: Schematic representation of the mechanisms of ROS-ERK pathway in urinary protein-induced injury in TECs. Urinary protein-induced ROS production triggers a cascade of phosphorylation reactions in the ERK pathway, which is a common mediator of protective autophagy and injury in TECs. In the early phase, cytoplasm p-ERK induces autophagy-associated adaptive response. Once stimulation is sustained, cytoplasm p-ERK transfers into the nucleus and elicits cell death.

the decreased expression of p62 indicates that autophagy degradation is not affected by ERK pathway. Meanwhile, the accumulation of LC3-II suggests autophagy is activated [14]. However, the increased dose of LC3-II was reverted and p62 returned to normal levels under stimulation of U0126, which inhibited ERK pathway effectively. These results reveal that the activation of autophagy induced by urinary proteins is at least partially dependent on the ERK pathway. An increasing number of articles have confirmed the truth that increasing autophagy in cells influenced by pathogenic factors could partially combat cellular injury and increase the cell survival rate [31, 32]. Consistent with the previous studies, when

autophagic flux was promoted by rapamycin, KIM-1 and NGAL excretion decreased despite of the increasing cell proliferation. Meanwhile, cellular injury tended to be aggravated when the autophagic pathway was blocked by chloroquine. Therefore, our results suggest that the activation of ERK pathway roused adaptive autophagic response under urinary protein stimulation.

Researchers reported that the apoptotic behavior of cells depend on the sustained activation of ERK within a certain period of time [33], and apoptosis could be aggravated when signals of activated ERK was delivered to the nucleus [34]. Specifically, the ERK activated messages in cytoplasm would induce autophagy [17]. Thus, we believe that when stimulated by urinary proteins, ERK pathway in the cytoplasm will activate an autophagy-related pathway and initiate an autophagy-associated adaptive response. However, under sustained stimulation of urinary proteins, the signals of activated ERK in the cytoplasm is likely to reenter the nucleus. This may attenuate autophagy and the ability of the cells to resist injury. In addition, the activated ERK in the nucleus will contact apoptosis-related pathways and result in cell apoptosis. In the absence of external interventions, persistent urinary proteins will eventually damage the TECs via the ERK pathway. In all, the results above suggest that the exact regulation of activation time and/or location of ERK pathway might offer a novel therapeutic opportunity in almost all the primary and secondary nephropathies with excessive urinary proteins, especially in diabetic nephropathy. However, the results of this study are still not enough to explain the role and mechanism of the ERK pathway in TECs. For example, scaffold proteins can accelerate the activation of this pathways and then participate in the regulation of the signal sustainability and intensity [35]. Hence, further information is required to explain the ERK pathway.

5. Conclusion

In summary, our work suggests that the ROS-ERK pathway is a double-edged sword when stimulated by urinary proteins. It can induce TEC injury and in the meantime provide an autophagy-associated adaptive response (Figure 5). Thus, the accurate regulation of this pathway is likely to be a promising target for patients suffer from TEC injury induced by urinary proteins.

Abbreviations

ERK: Extracellular signal-regulated protein kinases
 KIM-1: Kidney injury molecule-1
 NGAL: Neutrophil gelatinase-associated lipocalin
 ROS: Cellular reactive oxygen species
 TECs: Renal tubular epithelial cells
 LC3: Microtubule-associated protein 1 light chain 3
 NAC: N-acetylcysteine
 CAT: Catalase
 RAP: Rapamycin
 CQ: Chloroquine
 CON: Control

UP: Urinary proteins.

Data Availability

The datasets used and/or analyzed during the current study are available from the corresponding author on reasonable request.

Conflicts of Interest

The authors declare that they have no competing interests.

Authors' Contributions

Jian-kun Deng and Xueqin Zhang have contributed equally to this work.

Acknowledgments

This study was supported by the National Major Scientific and Technological Special Project for "Significant New Drugs Development" (grant no. 2017ZX09304019) and National Natural Science Foundation of China (Nos. 81570656, 81670654, and 81874443).

References

- [1] L. S. Gewin, "Renal fibrosis: primacy of the proximal tubule," *Matrix Biology*, vol. 68-69, pp. 248-262, 2018.
- [2] B. C. Liu, T. T. Tang, and L. L. Lv, "How tubular epithelial cell injury contributes to renal fibrosis," *Advances in Experimental Medicine and Biology*, vol. 1165, pp. 233-252, 2019.
- [3] B. C. Liu, T. T. Tang, L. L. Lv, and H. Y. Lan, "Renal tubule injury: a driving force toward chronic kidney disease," *Kidney International*, vol. 93, no. 3, pp. 568-579, 2018.
- [4] W. J. Liu, B. H. Xu, L. Ye et al., "Urinary proteins induce lysosomal membrane permeabilization and lysosomal dysfunction in renal tubular epithelial cells," *American Journal of Physiology. Renal Physiology*, vol. 308, no. 6, pp. F639-F649, 2015.
- [5] W. J. Liu, M.-N. Luo, J. Tan et al., "Autophagy activation reduces renal tubular injury induced by urinary proteins," *Autophagy*, vol. 10, no. 2, pp. 243-256, 2014.
- [6] J. Zhang, X. Wang, V. Vikash et al., "ROS and ROS-mediated cellular signaling," *Oxidative Medicine and Cellular Longevity*, vol. 2016, Article ID 4350965, 18 pages, 2016.
- [7] Y. Son, S. Kim, H. T. Chung, and H. O. Pae, "Reactive oxygen species in the activation of MAP kinases," *Methods in Enzymology*, vol. 528, pp. 27-48, 2013.
- [8] K. Kurtzeborn, H. N. Kwon, and S. Kuure, "MAPK/ERK signaling in regulation of renal differentiation," *International Journal of Molecular Sciences*, vol. 20, no. 7, p. 1779, 2019.
- [9] Y. Sun, W. Z. Liu, T. Liu, X. Feng, N. Yang, and H. F. Zhou, "Signaling pathway of MAPK/ERK in cell proliferation, differentiation, migration, senescence and apoptosis," *Journal of Receptor and Signal Transduction Research*, vol. 35, no. 6, pp. 600-604, 2015.
- [10] Z. Yang and D. J. Klionsky, "Mammalian autophagy: core molecular machinery and signaling regulation," *Current Opinion in Cell Biology*, vol. 22, no. 2, pp. 124-131, 2010.
- [11] Z. Y. Wu, C. L. Chiu, E. Lo, Y. R. J. Lee, S. Yamada, and S. H. Lo, "Hyperactivity of Mek in TNS1 knockouts leads to

- potential treatments for cystic kidney diseases,” *Cell Death & Disease*, vol. 10, no. 12, p. 871, 2019.
- [12] Z. Hui, Z. Jiang, D. Qiao et al., “Increased expression of LCN2 formed a positive feedback loop with activation of the ERK pathway in human kidney cells during kidney stone formation,” *Scientific Reports*, vol. 10, no. 1, p. 21287, 2020.
- [13] C. H. Weng, Y. J. Li, H. H. Wu et al., “Interleukin-17A induces renal fibrosis through the ERK and Smad signaling pathways,” *Biomedicine & Pharmacotherapy*, vol. 123, p. 109741, 2020.
- [14] Y. Wu, L. Wang, D. Deng, Q. Zhang, and W. Liu, “Renalase protects against renal fibrosis by inhibiting the activation of the ERK signaling pathways,” *International Journal of Molecular Sciences*, vol. 18, no. 5, p. 855, 2017.
- [15] H. Reich, D. Tritschler, A. M. Herzenberg et al., “Albumin activates ERK via EGF receptor in human renal epithelial cells,” *Journal of the American Society of Nephrology*, vol. 16, no. 5, pp. 1266–1278, 2005.
- [16] O. Takase, A. W. M. Minto, T. S. Puri et al., “Inhibition of NF- κ B-dependent Bcl-xL expression by clusterin promotes albumin-induced tubular cell apoptosis,” *Kidney International*, vol. 73, no. 5, pp. 567–577, 2008.
- [17] X. Li, A. Ma, and K. Liu, “Geniposide alleviates lipopolysaccharide-caused apoptosis of murine kidney podocytes by activating Ras/Raf/MEK/ERK-mediated cell autophagy,” *Artificial Cells, Nanomedicine, and Biotechnology*, vol. 47, no. 1, pp. 1524–1532, 2019.
- [18] R. Tang, C. Yang, J.-L. Tao et al., “Epithelial-mesenchymal transdifferentiation of renal tubular epithelial cells induced by urinary proteins requires the activation of PKC- α and β I isozymes,” *Cell Biology International*, vol. 35, no. 9, pp. 953–959, 2011.
- [19] S. Y. Shin and L. K. Nguyen, “Dissecting cell-fate determination through integrated mathematical modeling of the ERK/MAPK signaling pathway,” *Methods in Molecular Biology*, vol. 1487, pp. 409–432, 2017.
- [20] D. Bhatia, A. Capili, and M. E. Choi, “Mitochondrial dysfunction in kidney injury, inflammation, and disease: potential therapeutic approaches,” *Kidney Research and Clinical Practice*, vol. 39, no. 3, pp. 244–258, 2020.
- [21] G. Nowak, G. L. Clifton, M. L. Godwin, and D. Bakajsova, “Activation of ERK1/2 pathway mediates oxidant-induced decreases in mitochondrial function in renal cells,” *American Journal of Physiology. Renal Physiology*, vol. 291, no. 4, pp. F840–F855, 2006.
- [22] S. Zhuang, Y. Yan, R. A. Daubert, J. Han, and R. G. Schnellmann, “ERK promotes hydrogen peroxide-induced apoptosis through caspase-3 activation and inhibition of Akt in renal epithelial cells,” *American Journal of Physiology. Renal Physiology*, vol. 292, no. 1, pp. F440–F447, 2007.
- [23] M. T. Lindenmeyer, M. P. Rastaldi, M. Ikehata et al., “Proteinuria and hyperglycemia induce endoplasmic reticulum stress,” *Journal of the American Society of Nephrology*, vol. 19, no. 11, pp. 2225–2236, 2008.
- [24] E. Erkan, P. Devarajan, and G. J. Schwartz, “Mitochondria are the major targets in albumin-induced apoptosis in proximal tubule cells,” *Journal of the American Society of Nephrology*, vol. 18, no. 4, pp. 1199–1208, 2007.
- [25] H. Lei and A. Kazlauskas, “Growth factors outside of the platelet-derived growth factor (PDGF) family employ reactive oxygen species/Src family kinases to activate PDGF receptor α and thereby promote proliferation and survival of cells,” *The Journal of Biological Chemistry*, vol. 284, no. 10, pp. 6329–6336, 2009.
- [26] A. León-Buitimea, L. Rodríguez-Fragoso, F. T. Lauer, H. Bowles, T. A. Thompson, and S. W. Burchiel, “Ethanol-induced oxidative stress is associated with EGF receptor phosphorylation in MCF-10A cells overexpressing CYP2E1,” *Toxicology Letters*, vol. 209, no. 2, pp. 161–165, 2012.
- [27] A. A. Deora, D. P. Hajjar, and H. M. Lander, “Recruitment and activation of Raf-1 kinase by nitric oxide-activated Ras,” *Biochemistry*, vol. 39, no. 32, pp. 9901–9908, 2000.
- [28] S. Cagnol and J. C. Chambard, “ERK and cell death: mechanisms of ERK-induced cell death—apoptosis, autophagy and senescence,” *The FEBS Journal*, vol. 277, no. 1, pp. 2–21, 2010.
- [29] J. Wang, M. W. Whiteman, H. Lian et al., “A non-canonical MEK/ERK signaling pathway regulates autophagy via regulating beclin 1,” *The Journal of Biological Chemistry*, vol. 284, no. 32, pp. 21412–21424, 2009.
- [30] Y. Zeng, X. Yang, J. Wang, J. Fan, Q. Kong, and X. Yu, “Aristolochic acid I induced autophagy attenuates cell apoptosis via ERK 1/2 pathway in renal tubular epithelial cells,” *PLoS One*, vol. 7, no. 1, article e30312, 2012.
- [31] N. Pallet, N. Bouvier, C. Legendre et al., “Autophagy protects renal tubular cells against cyclosporine toxicity,” *Autophagy*, vol. 4, no. 6, pp. 783–791, 2014.
- [32] G. P. Kaushal, “Autophagy protects proximal tubular cells from injury and apoptosis,” *Kidney International*, vol. 82, no. 12, pp. 1250–1253, 2012.
- [33] S. Cagnol, E. Van Obberghen-Schilling, and J. C. Chambard, “Prolonged activation of ERK1,2 induces FADD-independent caspase 8 activation and cell death,” *Apoptosis*, vol. 11, no. 3, pp. 337–346, 2006.
- [34] P. K. Wu, A. Becker, and J. I. Park, “Growth inhibitory signaling of the Raf/MEK/ERK pathway,” *International Journal of Molecular Sciences*, vol. 21, no. 15, p. 5436, 2020.
- [35] D. K. Morrison and R. J. Davis, “Regulation of MAP kinase signaling modules by scaffold proteins in mammals,” *Annual Review of Cell and Developmental Biology*, vol. 19, no. 1, pp. 91–118, 2003.